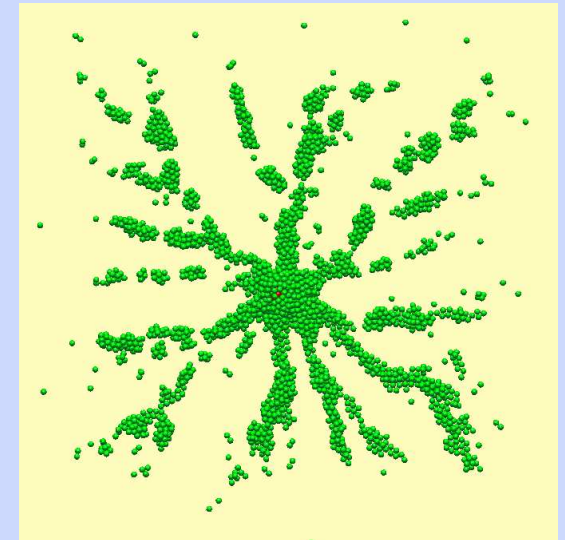
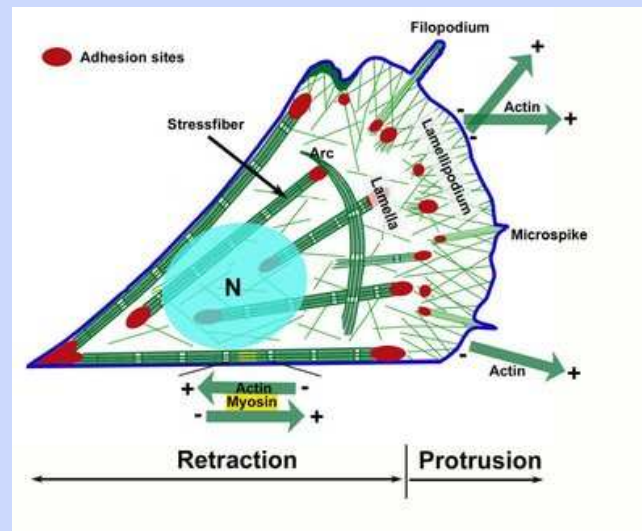
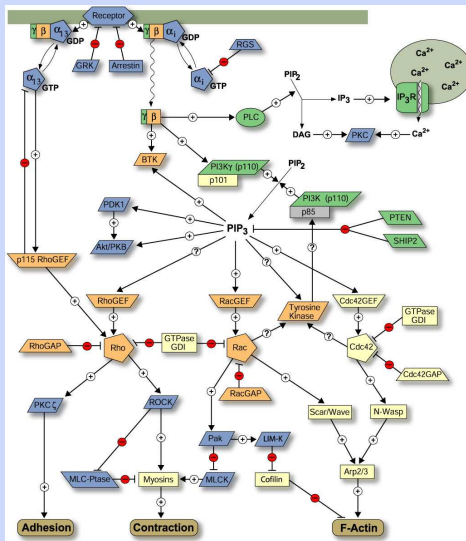


From Crawlers to Swimmers- Mathematical and Computational Problems in Cell Motility

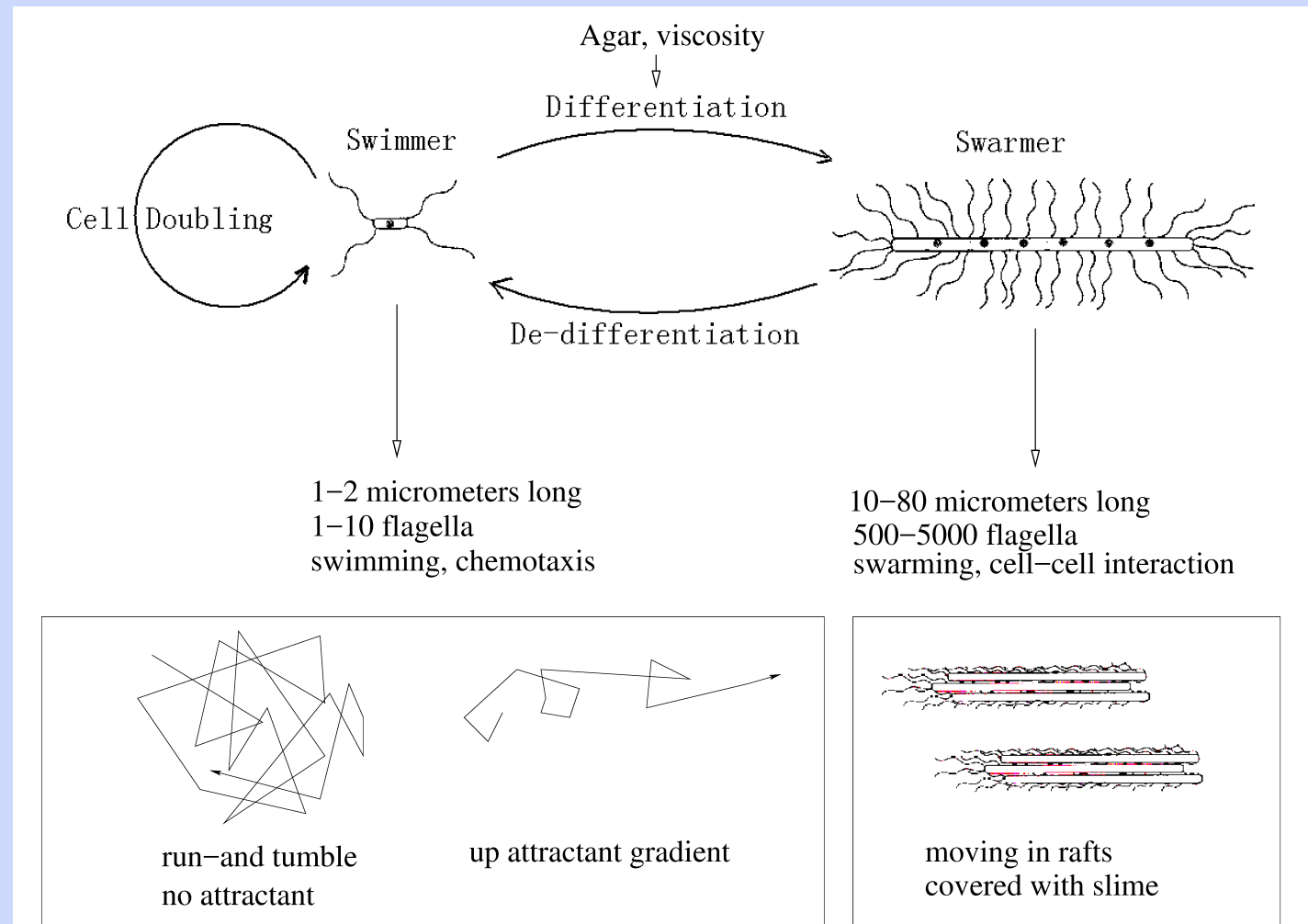
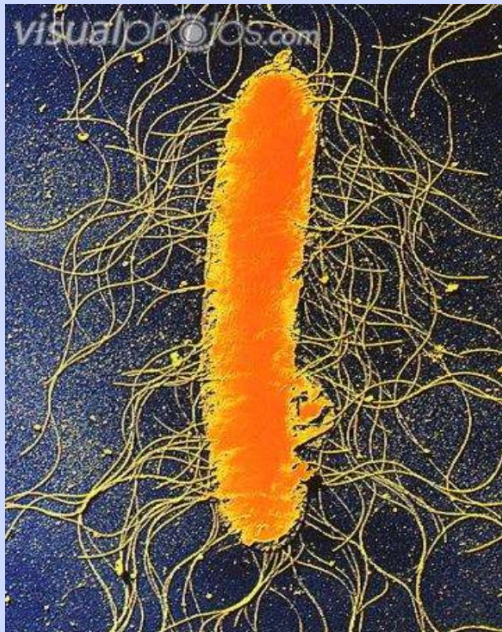
Hans G. Othmer
School of Mathematics
University of Minnesota



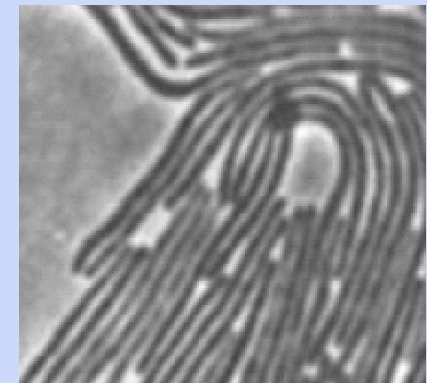
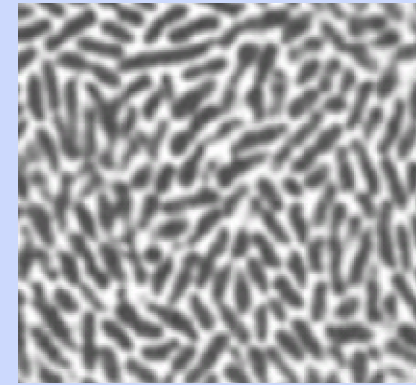
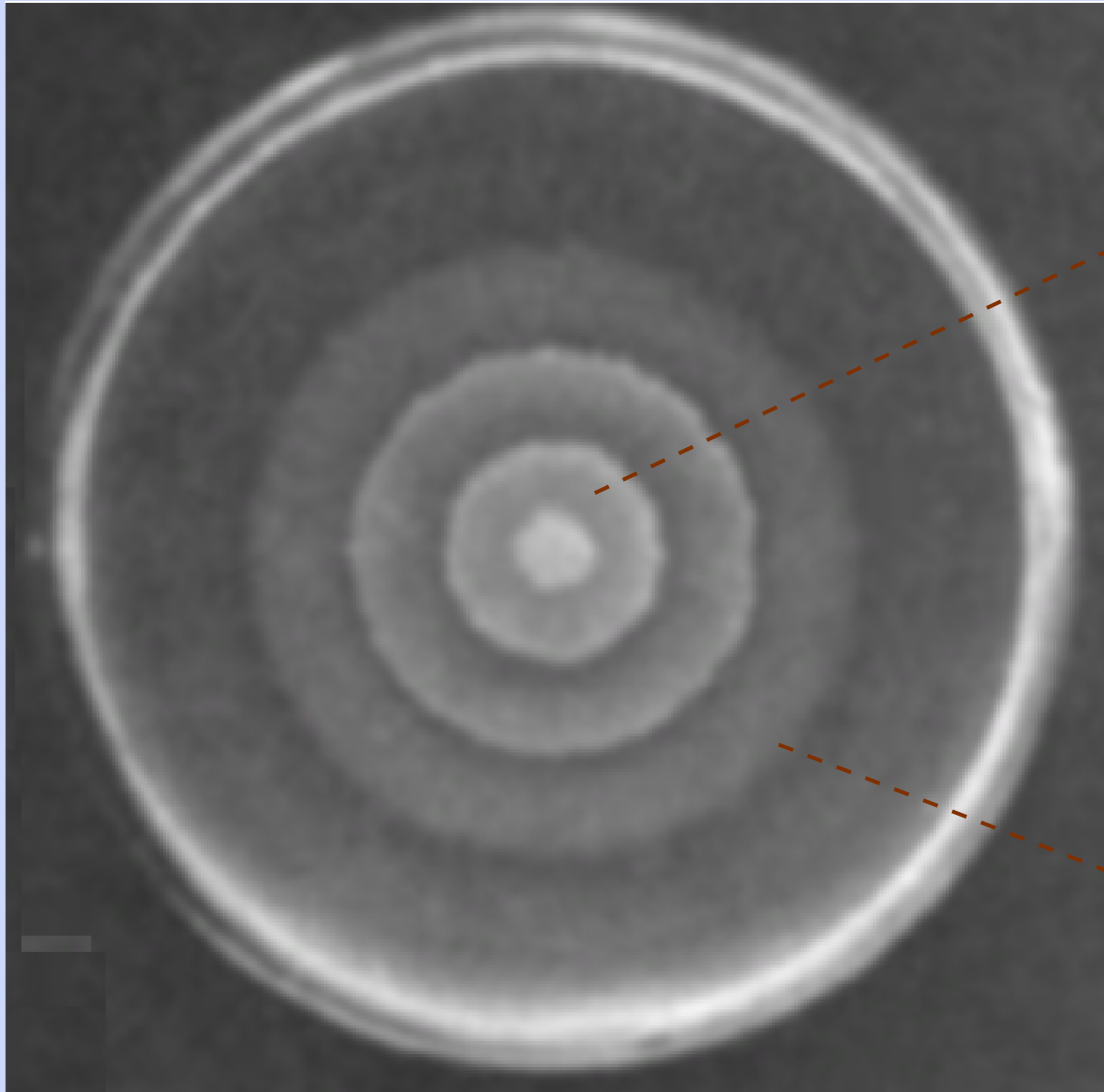
Edinburgh – Oct. 2017 – Lecture 4

Basic facts about *Proteus mirabilis*

- In liquid medium, *P. mirabilis* cells are predominantly swimmers.
- When inoculated on hard surfaces, swimmers differentiate into swarmer.

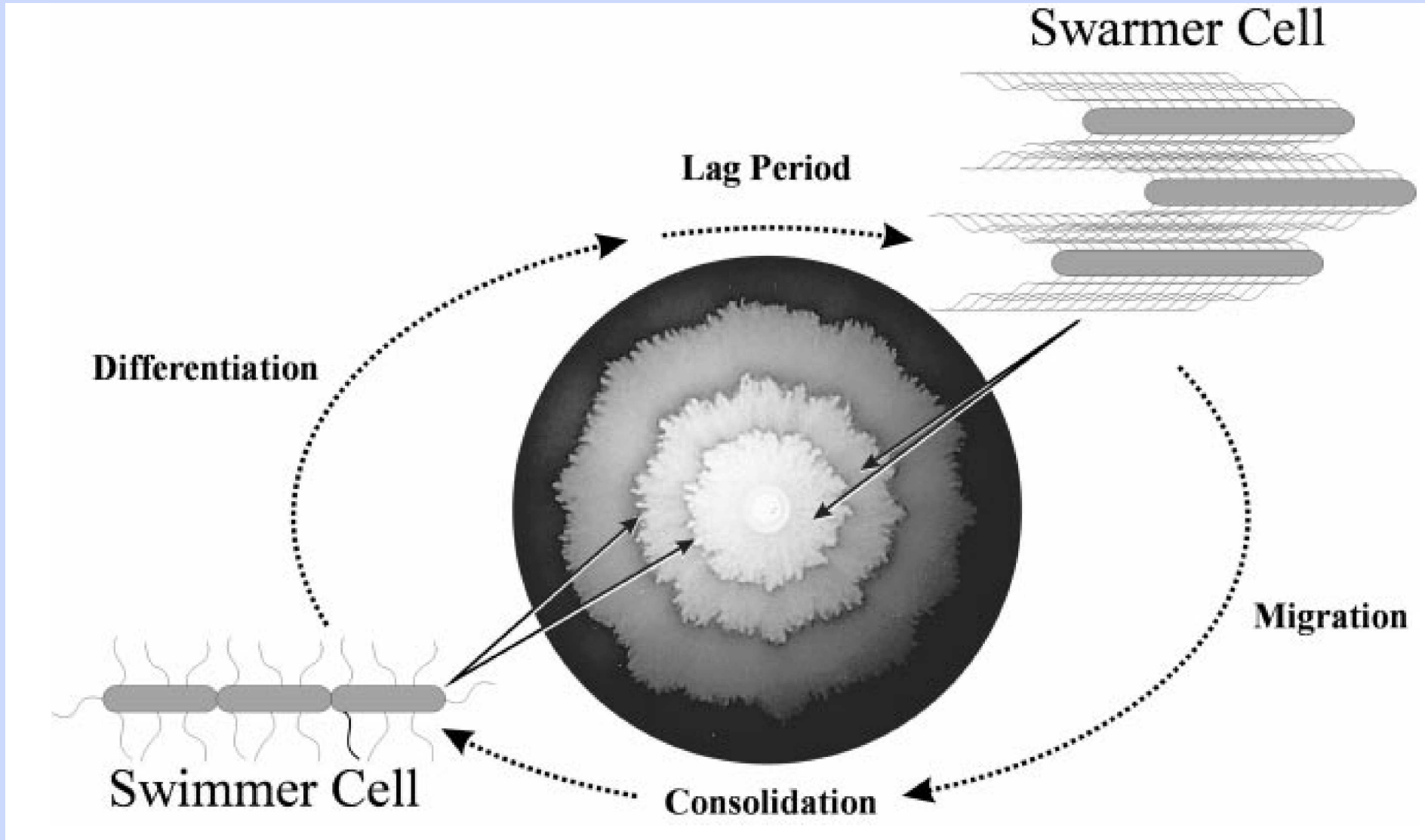


Pattern formation in *Proteus* on hard surfaces



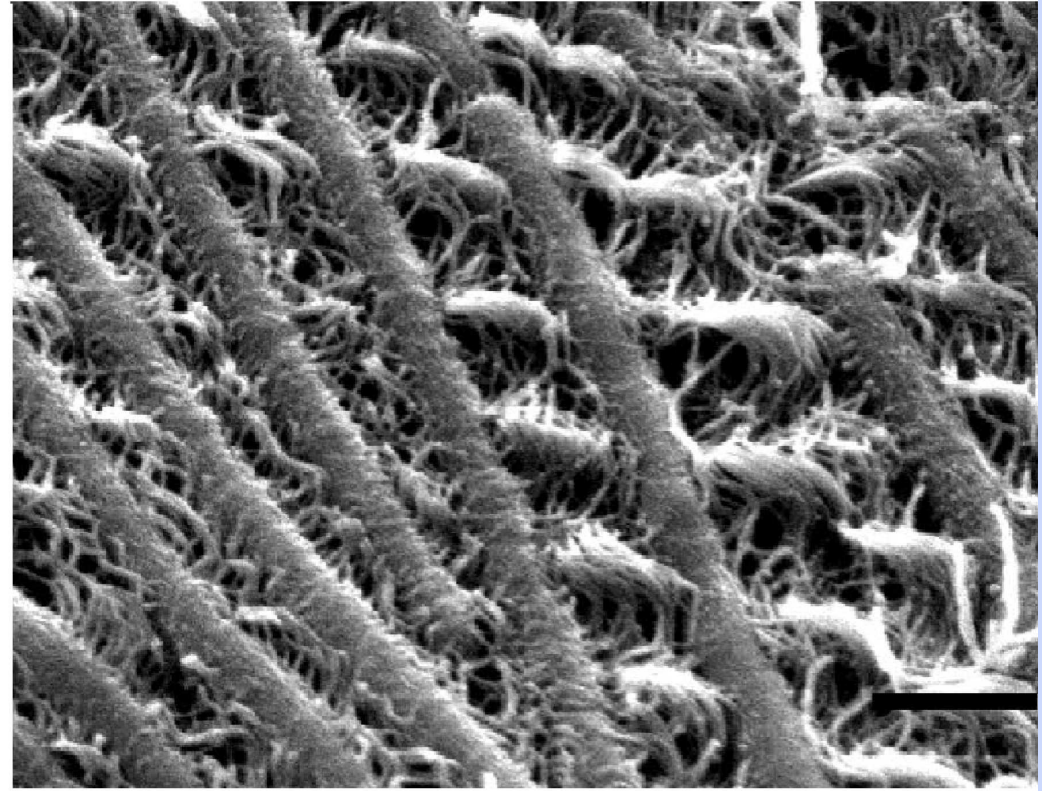
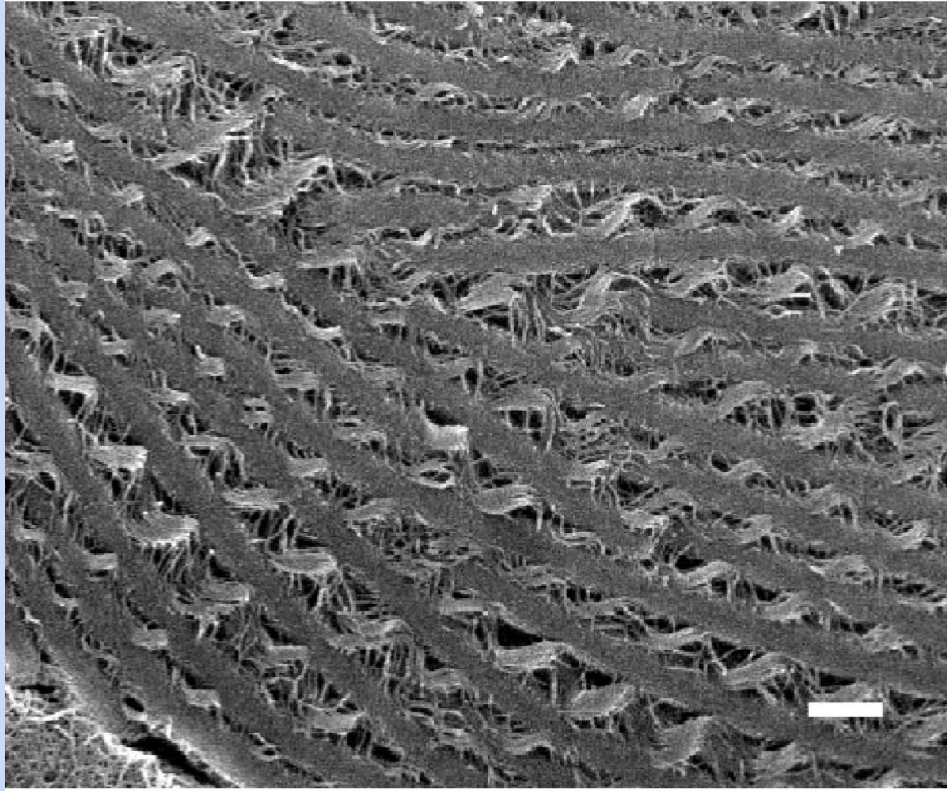
R. D. Williams. Ann. Rev. Microbiol. 1978. Rauprich *et al.* Periodic phenomena in *Proteus mirabilis* swarm colony de

The spatial variation of cell-level dynamics



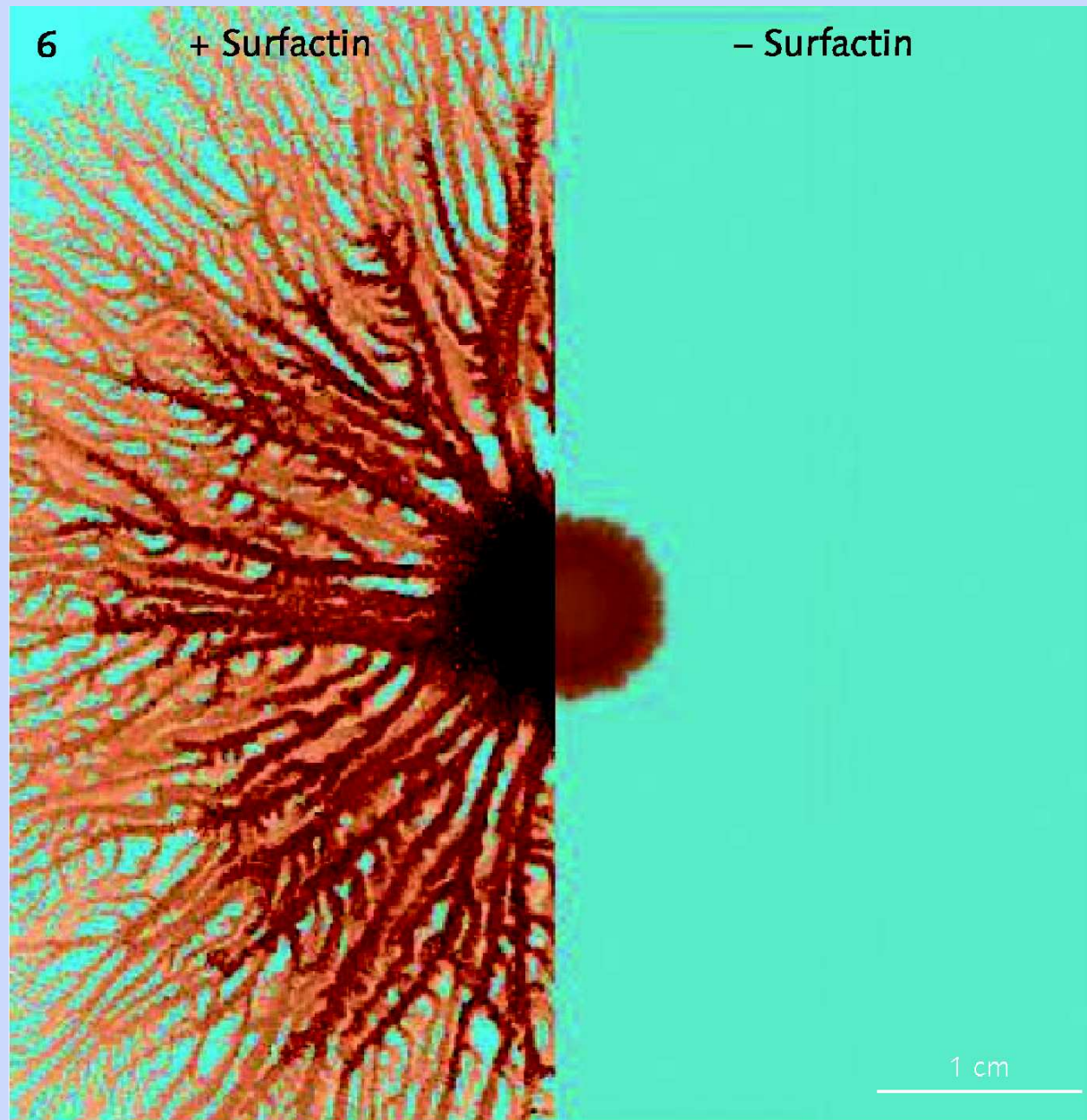
R. Schneider, et al., Detection and mutation of a luxS-encoded autoinducer in *Proteus mirabilis*, Microbiology, 2002.

A close-up of swarmers



B. V. Jones, et al., Ultrastructure of *Proteus mirabilis* Swarmer Cell Rafts and Role of Swarming in Catheter-Associated Urinary Tract Infection Infection and Immunity, 72, 3941, (2004).

Surface tension is important for spreading



Previous work on the front dynamics

S. Esipov and J. Shapiro. Kinetic model of *Proteus Mirabilis* swarm colony development. *J. Math. Biol.*, 36:249–268, 1998.

G. Medvedev, T. Kaper, and N. Kopell. A reaction-diffusion system with periodic front dynamics. *SIAM J. App. Math.*, 60(5):1601–1638, 2000.

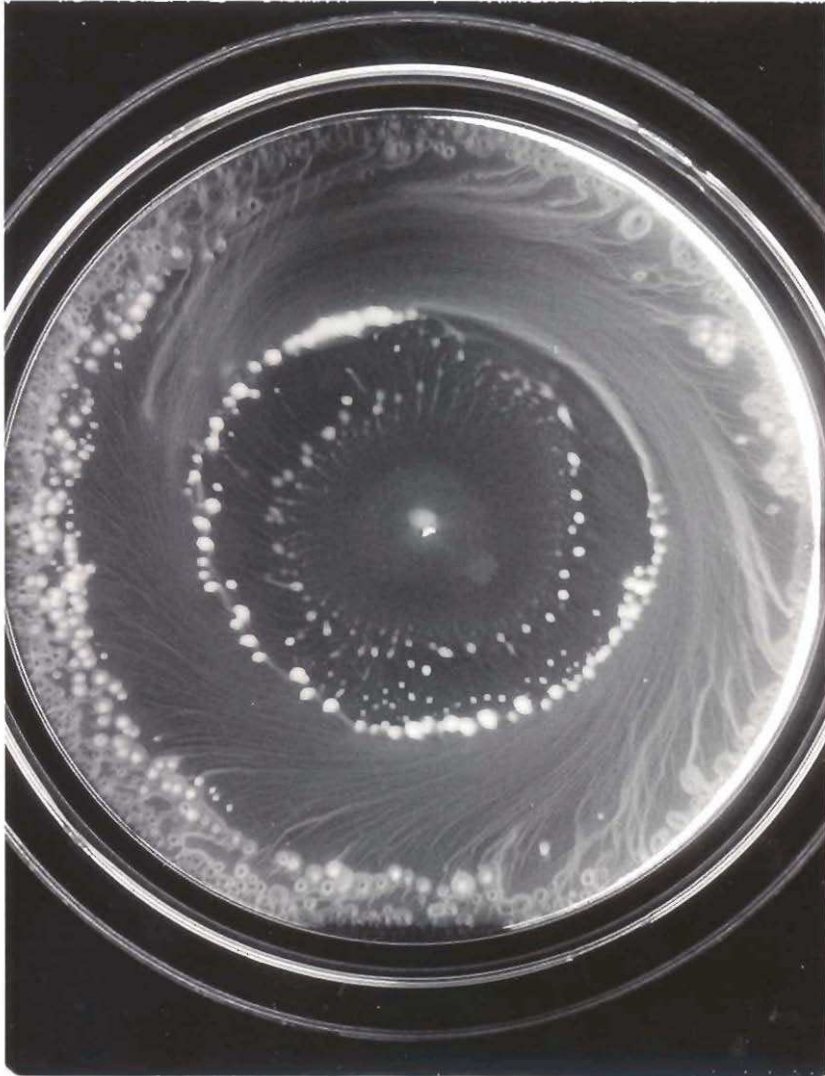
A. Czirók, M. Matsushita, and T. Vicsek. Theory of periodic swarming of bacteria: application to proteus mirabilis. *Phys Rev E Stat Nonlin Soft Matter Phys.*, 63, 2001.

B. Ayati. A structured-population model of *P. mirabilis* swarm-colony development. *J. Math. Bio.*, 52, 93, 2006.

B. Ayati. Modeling the role of the cell cycle in regulating *P. mirabilis* swarm-colony development. Preprint 2007.

M. A. Bees, et al, The interaction of thin-film flow, bacterial swarming and cell differentiation in colonies of *Serratia liquefaciens*, *J. Math. Biol.*, 40, 2000.

Experimental results on patterning in the core

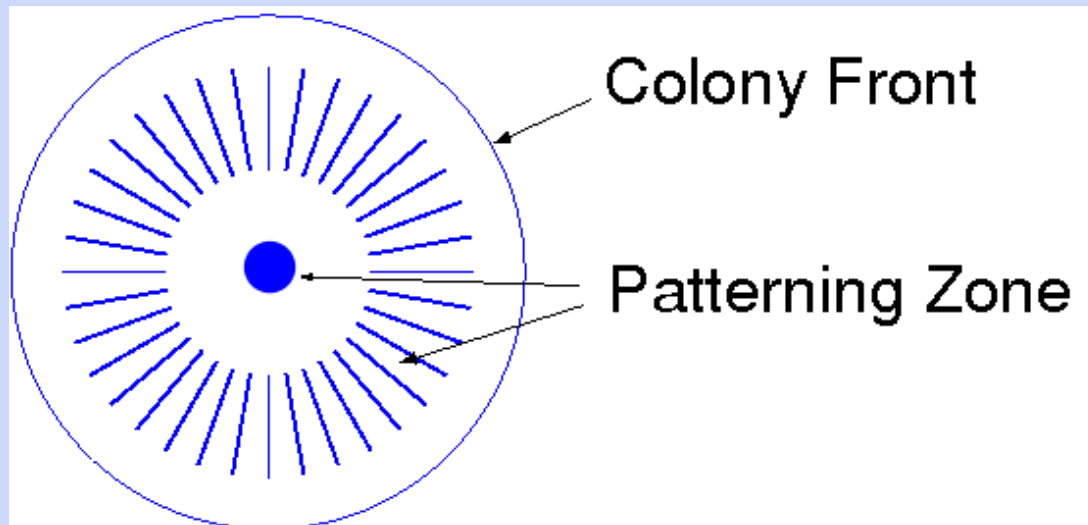


Photos courtesy of Elena Budrene

Spatial patterning in *Proteus mirabilis*

- We focus on the patterns generated by swimmers in the central area.

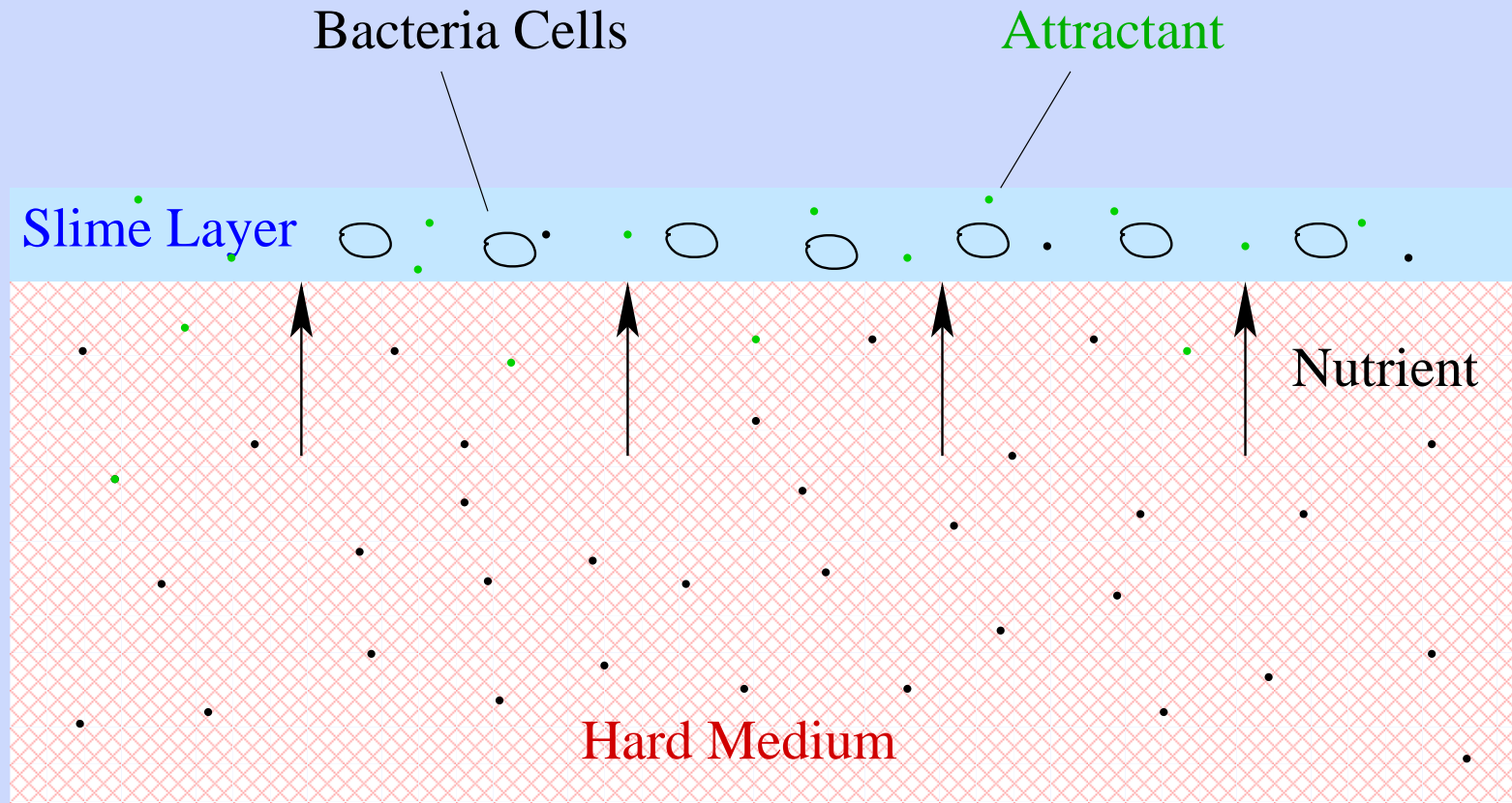
Top view



- Key features of these patterns:
 - ◆ the processes generating radial streams
 - ◆ the handedness of the spiral streams
 - ◆ the breakup of streams into 'trains'

- We assume:
 - ◆ cells in the patterning zone are swimmer cells,
 - ◆ swimmer cells secrete a chemoattractant and respond to it.

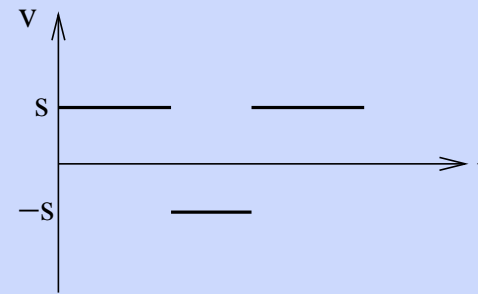
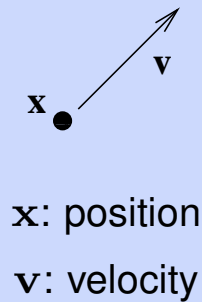
Side view



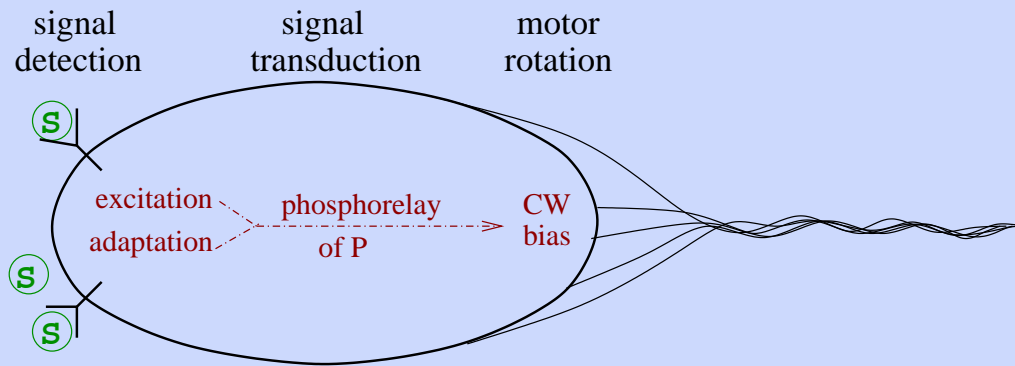
- We have developed both a hybrid cell-based model and a continuum model to incorporate these processes.

The hybrid cell-based model

- The movement of each cell is modeled by a velocity jump process.



- The turning rate is determined by a simplified single cell signal transduction model.



$$\frac{dy_1}{dt} = \frac{G(c(\mathbf{x}, t)) - (y_1 + y_2)}{t_e} \quad (1)$$

$$\frac{dy_2}{dt} = \frac{G(c(\mathbf{x}, t)) - y_2}{t_a}$$

$$\lambda = \lambda_0 \left(1 - \frac{y_1}{\gamma_0 + |y_1|} \right) \quad (2)$$

- A cell divides into two daughter cells every 2 hours.
- The attractant and nutrient concentrations are governed by

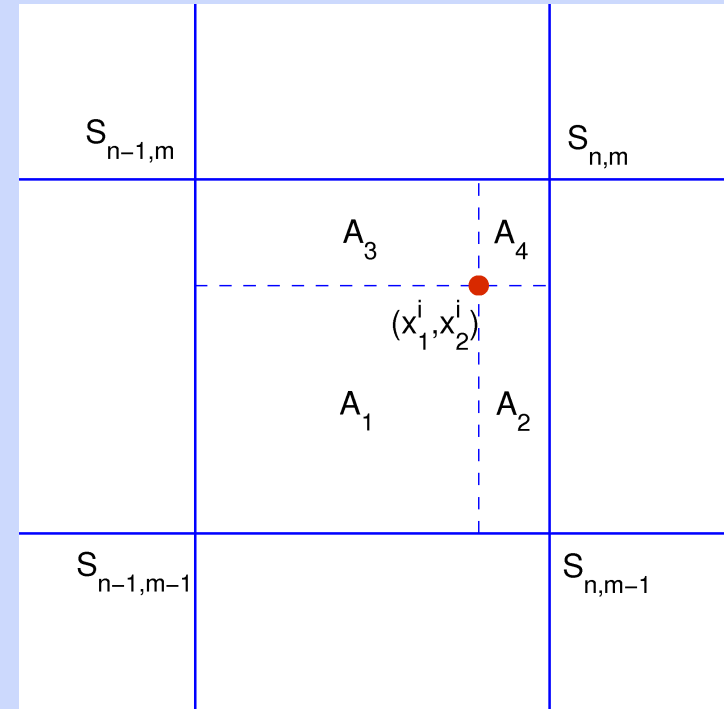
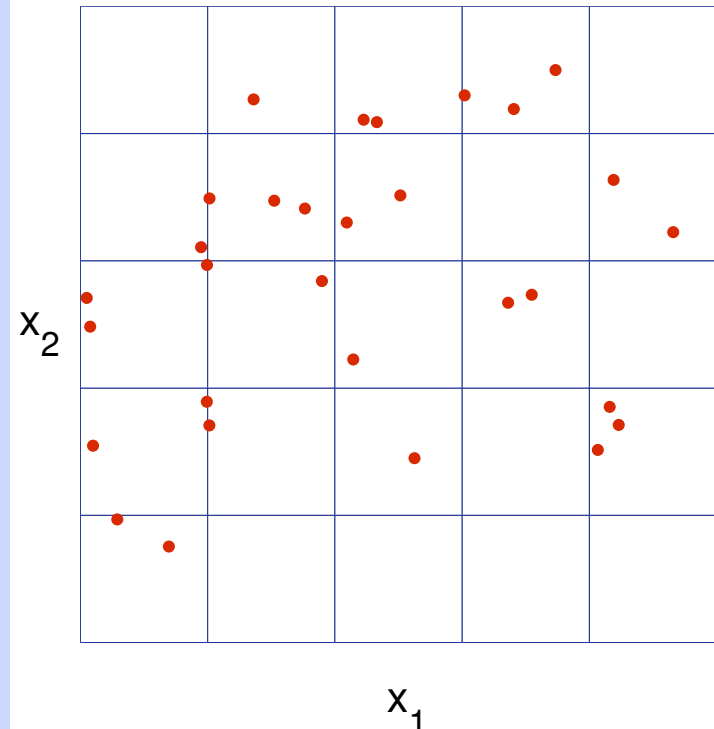
$$\begin{aligned}\frac{\partial c}{\partial t} &= D_c \Delta c + \text{secretion by cells} - \text{degradation} \\ \frac{\partial f}{\partial t} &= D_f \Delta f - \text{uptake by cells}\end{aligned}$$

If we assume constant rates,

$$\begin{aligned}\frac{\partial c}{\partial t} &= D_c \Delta c + \gamma \sum_{n=1}^N \delta(\mathbf{x} - \mathbf{x}^i) - \mu c \quad \text{in } D^2 \times \mathbb{R}^+ \\ \frac{\partial f}{\partial t} &= D_f \Delta c - k \sum_{n=1}^N \delta(\mathbf{x} - \mathbf{x}^i)) \quad \text{in } D^2 \times \mathbb{R}^+ \\ + \quad \text{Neumann BC: } &\frac{\partial c}{\partial n} = \frac{\partial f}{\partial n} = 0 \quad \text{in } \partial D^2 \times \mathbb{R}^+\end{aligned}$$

- The model was originally developed for *E. coli*, where it predicts very well the network and ring formation.

The computational algorithm



- We use the grid-to-cell interpolation \mathcal{T}_{gc} defined by the bilinear function:

$$\mathcal{T}_{gc}(x_1^i, x_2^i) = \frac{A_4}{A} c_{n-1,m-1} + \frac{A_3}{A} c_{n,m-1} + \frac{A_2}{A} c_{n-1,m} + \frac{A_1}{A} c_{n,m}$$

where $A = h_1 h_2$ and $A_i, i = 1, 2, 3, 4$ are the area fractions.

- Cell-to-grid transfer is done by area fractions

S1 Initialization.

(a) Initialize the chemical fields and the cell properties.

S2 For time step $l = 1, 2 \dots$, update the data for each cell.

(a) Determine the direction of movement θ_i by (2).

i) Generate a random number $r \in U[0, 1]$;

ii) If $r < \lambda^i * k$, update θ_i with a new random direction.

(b) $(x_i^1, x_i^2) \leftarrow (x_1^i + sk \cos \theta_i, x_2^i + sk \sin \theta_i)$. If (x_i^1, x_i^2) is outside the domain, reflect across the boundary.

(c) $T_l^i \leftarrow T_l^i + k$. If $T_l^i > 2$ hours, the cell divides into two daughter cells.

(d) Update (y_1^i, y_2^i) according to (1).

i) Determine the attractant level at the beginning of the step c_{old}^i and after the cell moves c_{new}^i .

ii) Estimate the attractant level during the movement by $c(t) = c_{old}^i \frac{t - lk}{k} + c_{new}^i \frac{lk + k - t}{k}$ and integrate the y_2 equation to get y_2^i .

iii) $y_1^i \leftarrow G(c) - y_2^i$.

S3 Compute the source term of the attractant due to the secretion by the cells

$$f^l = \gamma k \sum_{i=1}^N \delta(\mathbf{x} - \mathbf{x}^i).$$

S4 For the PDEs use the ADI scheme

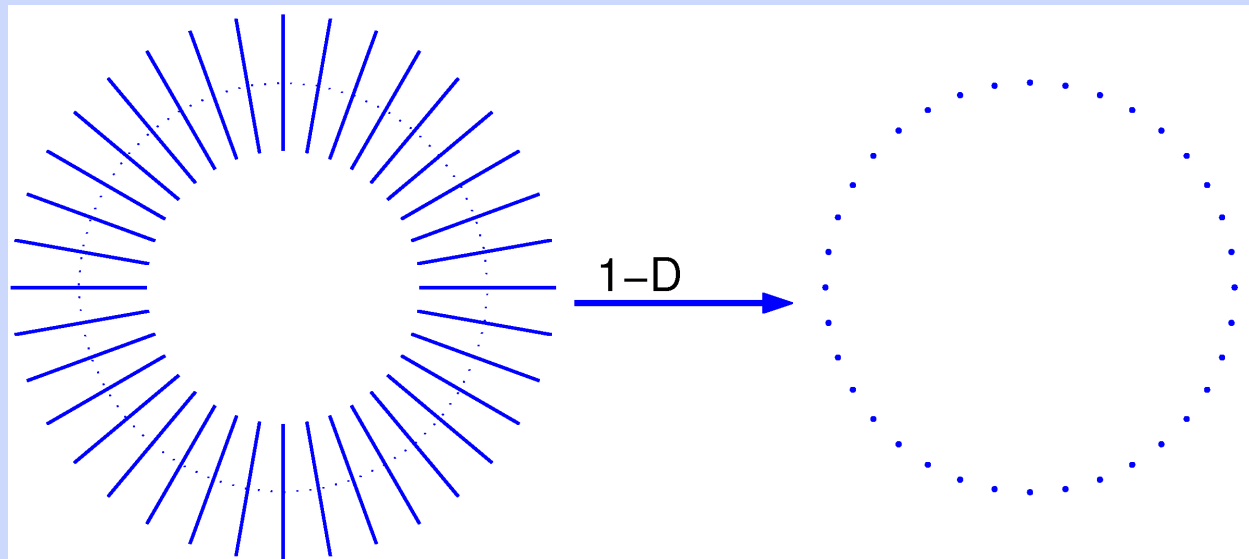
$$\begin{aligned} \frac{c_{n,m}^{l+1/2} - c_{n,m}^l}{k/2} &= D \frac{c_{n+1,m}^{l+1/2} - 2c_{n,m}^{l+1/2} + c_{n-1,m}^{l+1/2}}{h_x^2} \\ &\quad + D \frac{c_{n,m+1}^l - 2c_{n,m}^l + c_{n,m-1}^l}{h_x^2} - \gamma \frac{c_{nm}^l + c_{nm}^{l+1/2}}{2} + f^l \\ \frac{c_{n,m}^{l+1} - c_{n,m}^{l+1/2}}{k/2} &= D \frac{c_{n+1,m}^{l+1/2} - 2c_{n,m}^{l+1/2} + c_{n-1,m}^{l+1/2}}{h_x^2} \\ &\quad + D \frac{c_{n,m+1}^{l+1} - 2c_{n,m}^{l+1} + c_{n,m-1}^{l+1}}{h_x^2} - \gamma \frac{c_{nm}^{l+1/2} + c_{nm}^{l+1}}{2} + f^l \end{aligned}$$

with Neumann data on the boundary

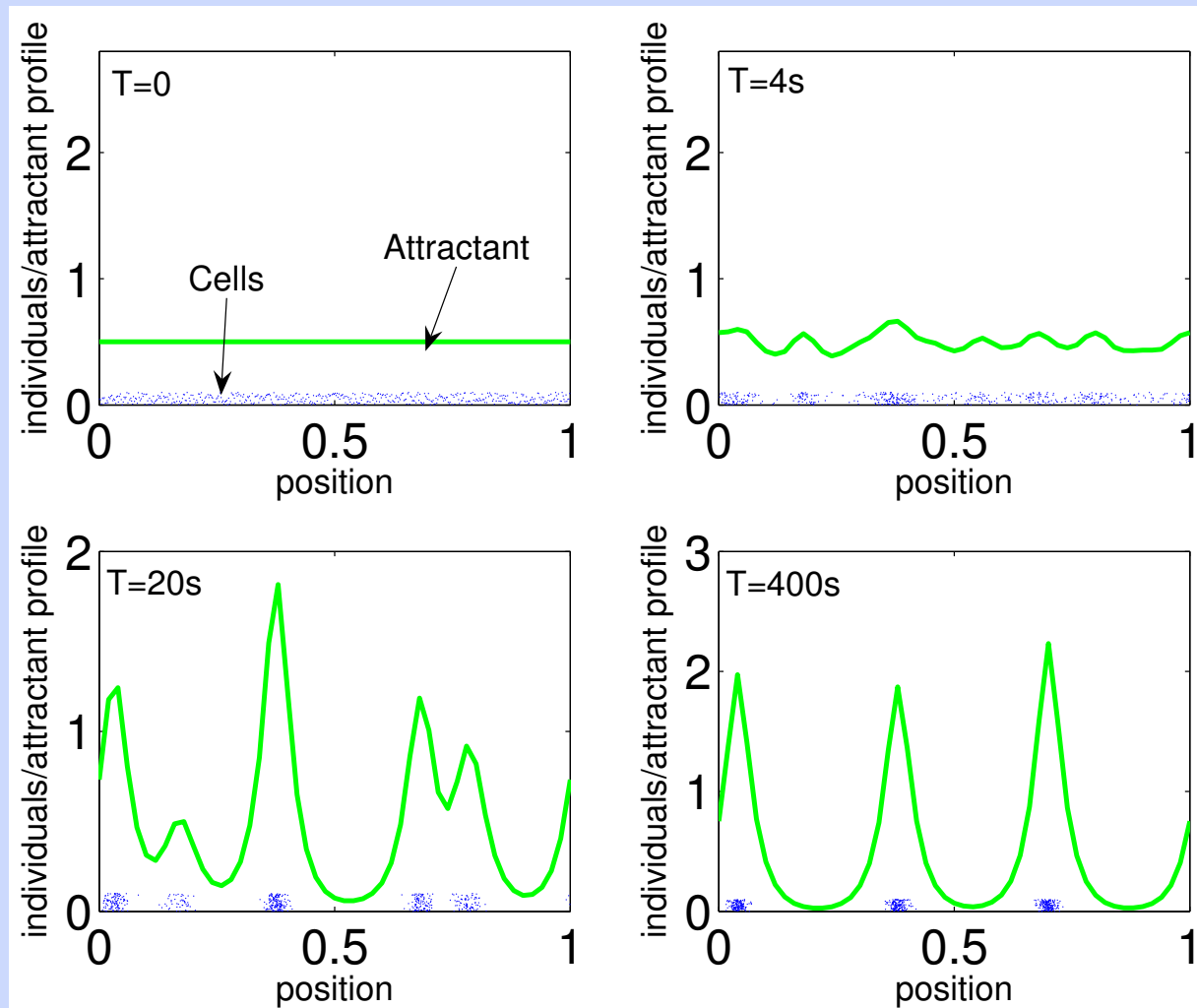
Step 1: radial streams

- Cell growth is neglected (radial streams appear in minutes compared with a doubling time of 2 hours).
- As a result, the nutrient equation is uncoupled from the system.
- First consider a 1-D circular section of the region; then streams reduce to aggregates on a circle.

1-D section



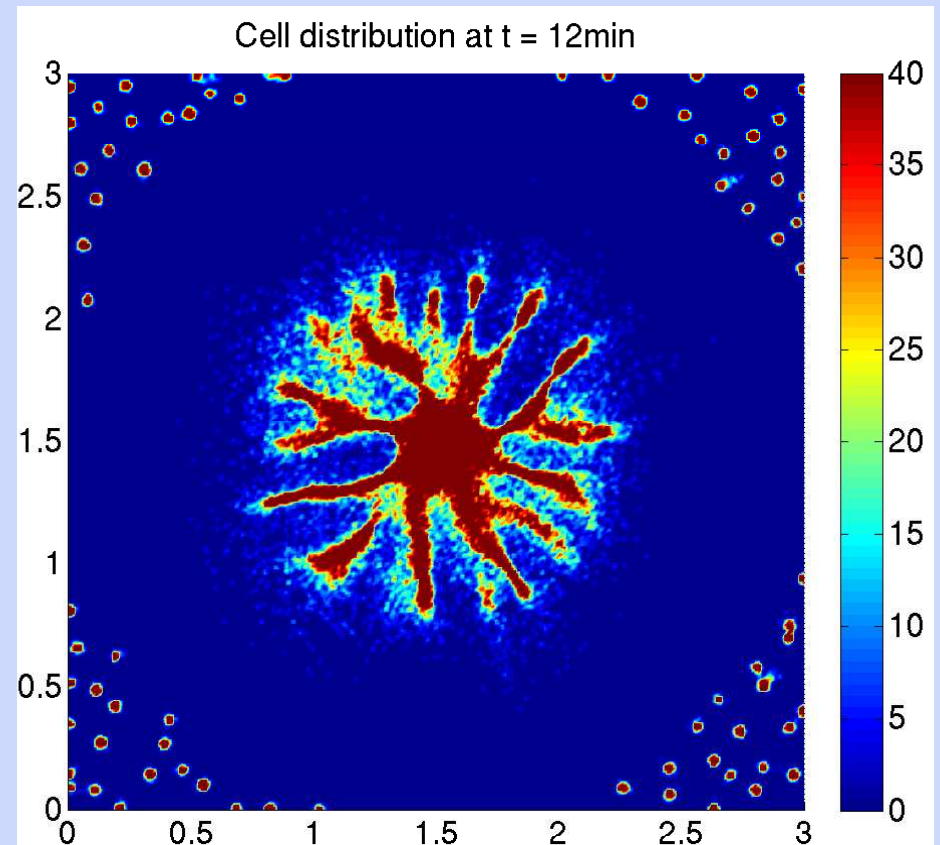
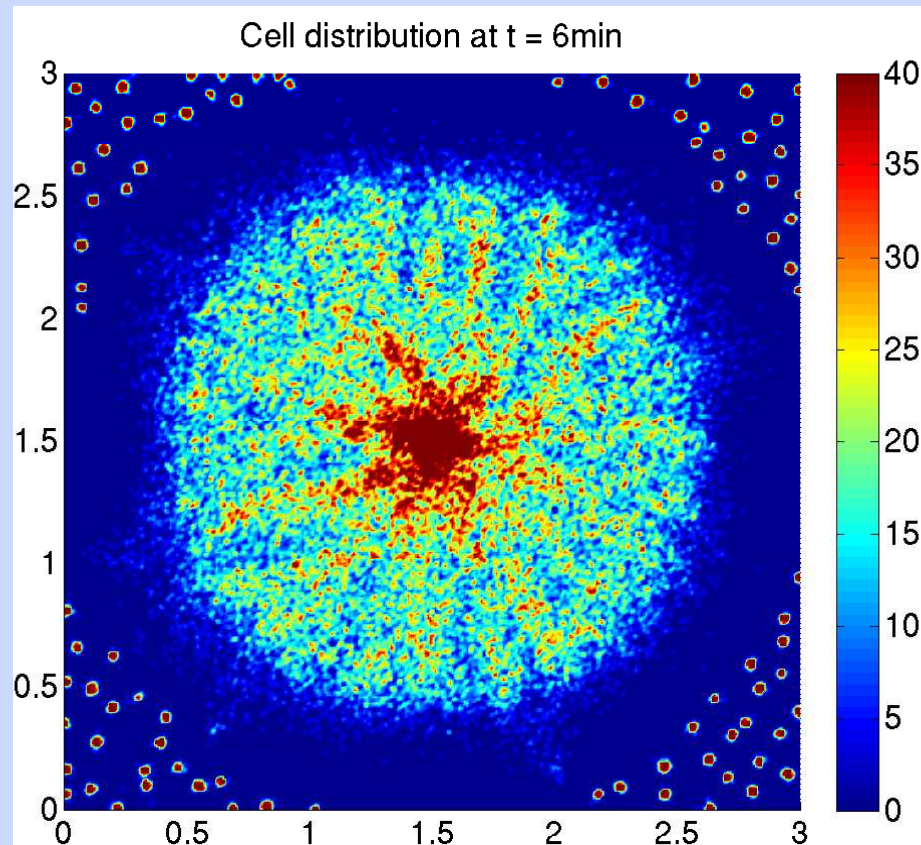
Numerical results for 500 cells on the interval



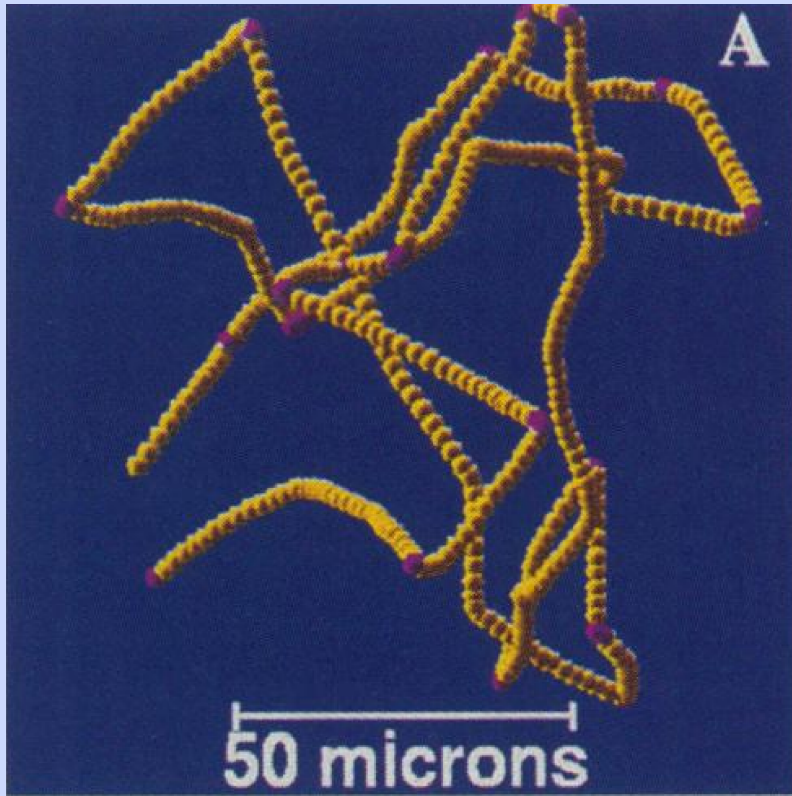
One can understand this using a macroscopic model with chemotaxis – see Xue and Othmer (2007).

Parameters used are: $s = 20\mu\text{m/s}$, $\lambda_0 = 1/\text{s}$, $D_c = 10^{-5}\text{cm}^2/\text{s}$, $\gamma = 1 \times 10^{-2}$, $\mu = 1 \times 10^{-3}$, $\gamma_0 = 0.1$, $L = 1\text{ cm}$, $G(c) = c$, $t_a = 5\text{ s}$.

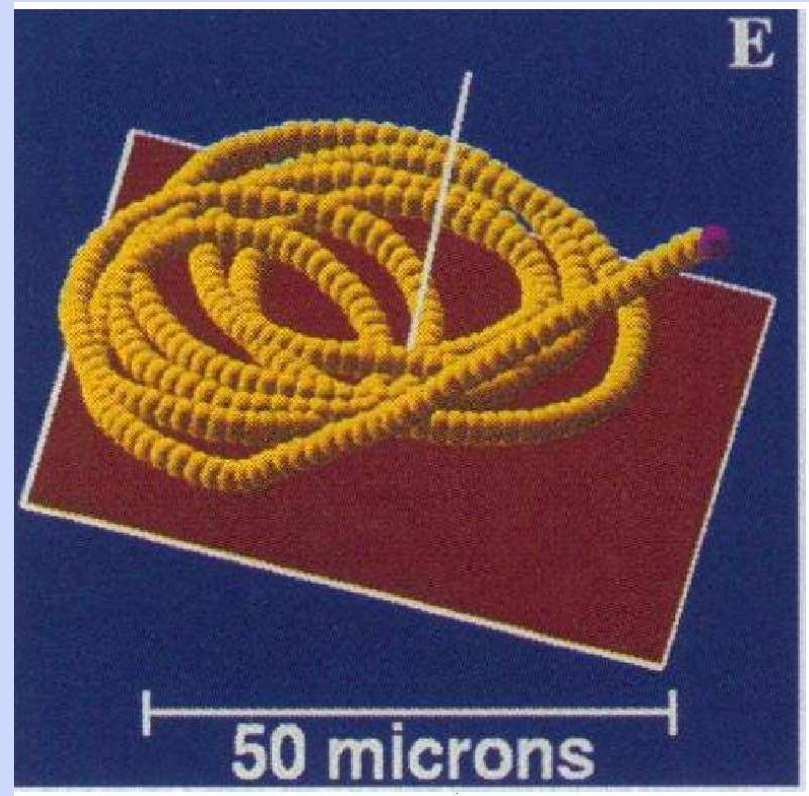
Numerical results in 2D



Cell tracks: the effect of the boundary



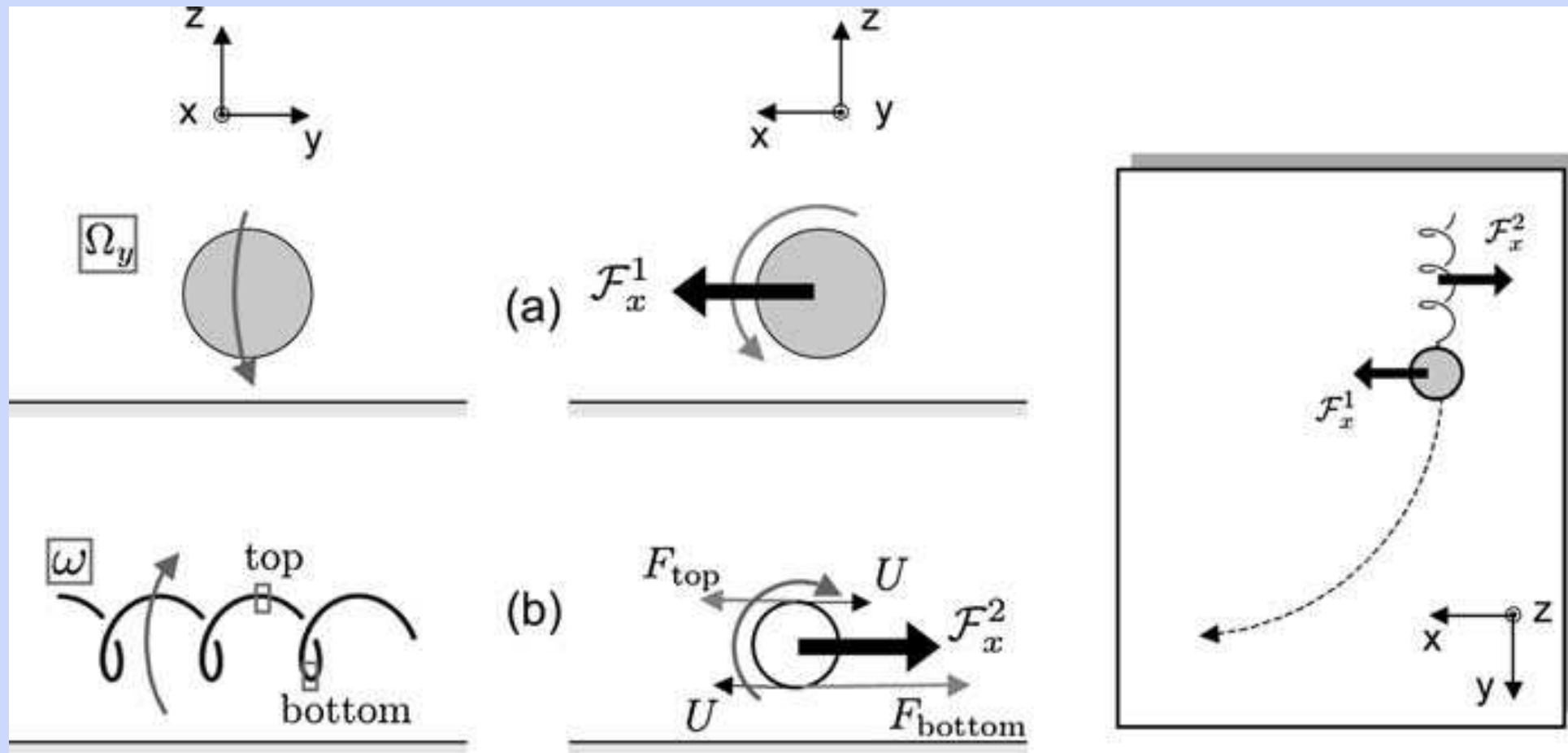
A track far from the surface



A track near the surface

Frymier *et. al.*, Three-dimensional tracking of motile bacteria near a solid planar surface, PNAS, 92, 1995

The physical picture



The mechanics with boundary effects

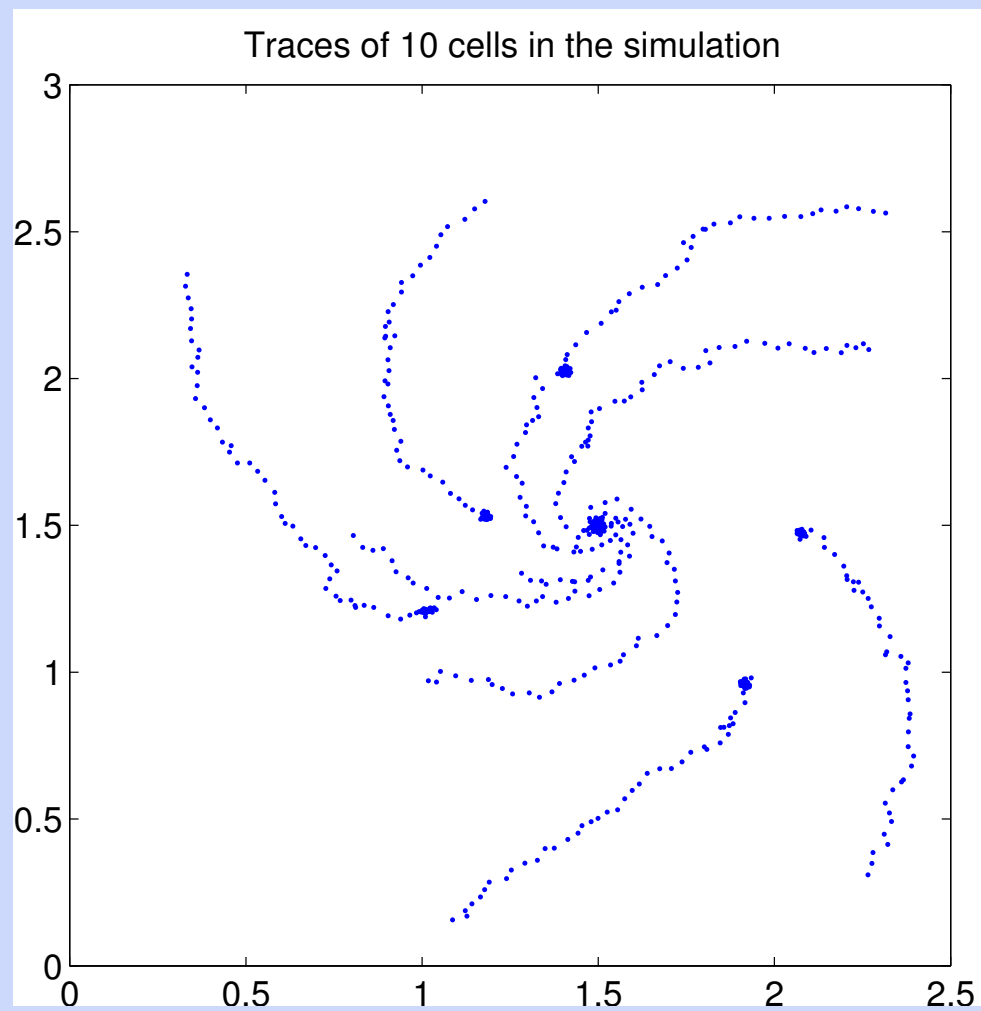
- Incompressible Newtonian fluid with constant density:

$$\nabla \cdot \mathbf{u} = 0$$
$$\frac{\partial \mathbf{u}}{\partial t} + \mathbf{u} \cdot \nabla \mathbf{u} = \mathbf{f} - \frac{1}{\rho} \nabla p + \nu \nabla^2 \mathbf{u}$$

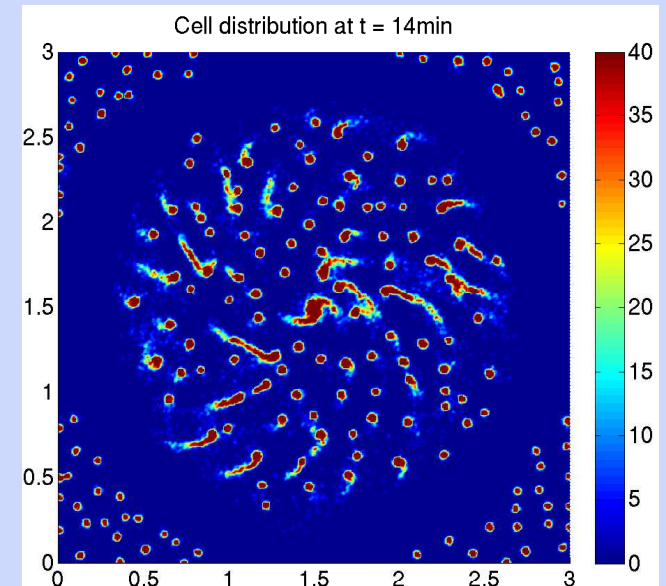
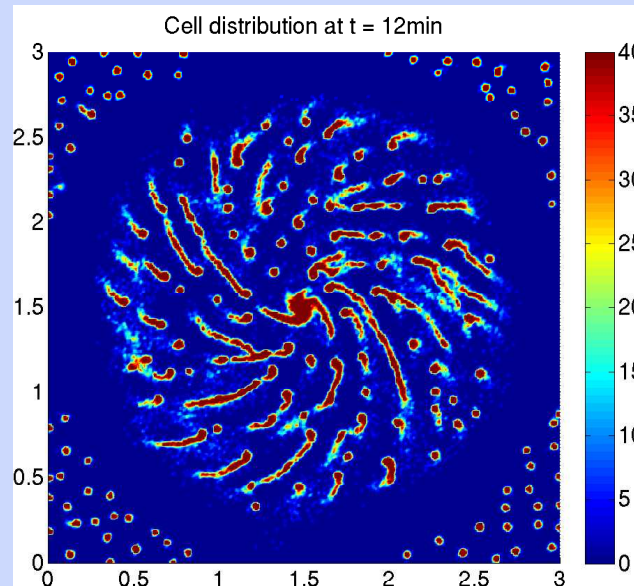
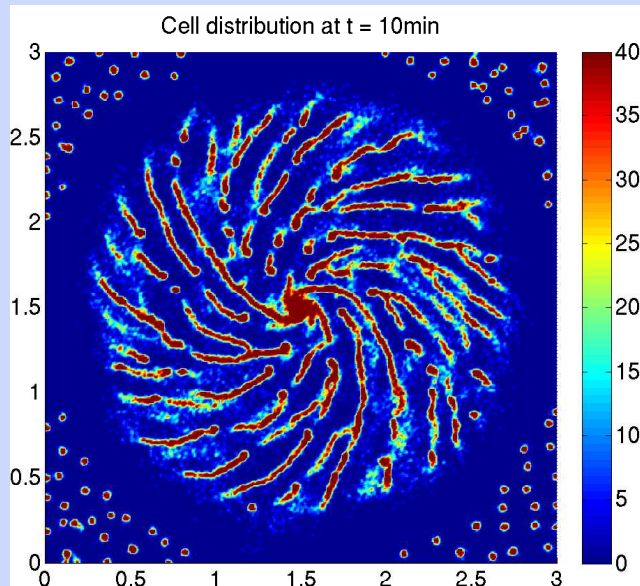
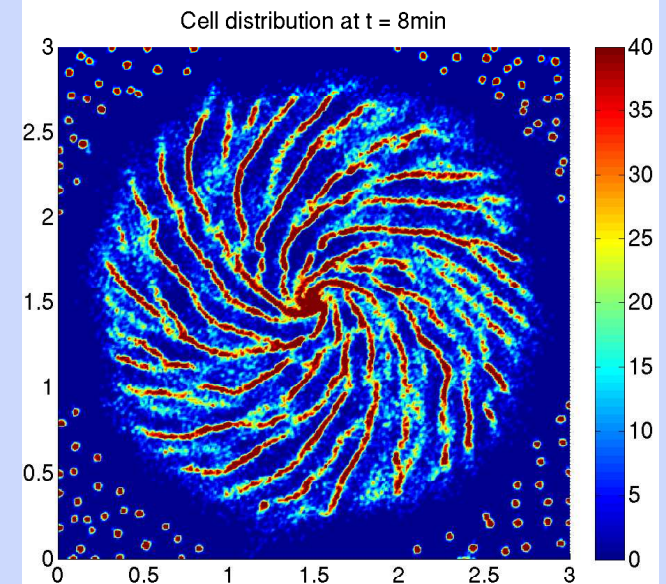
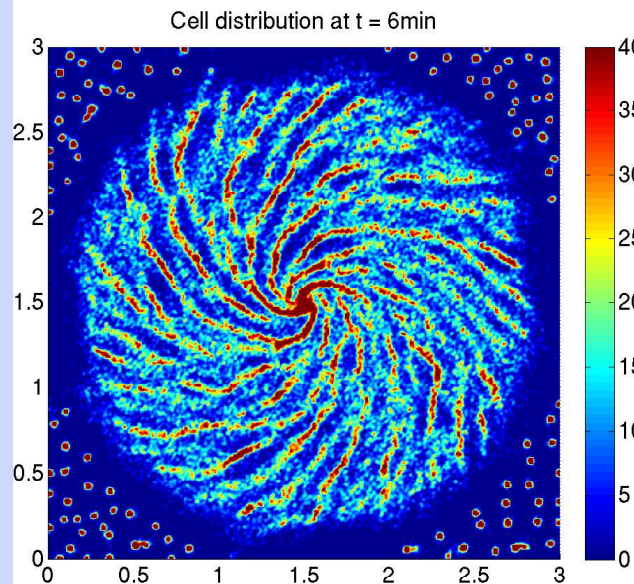
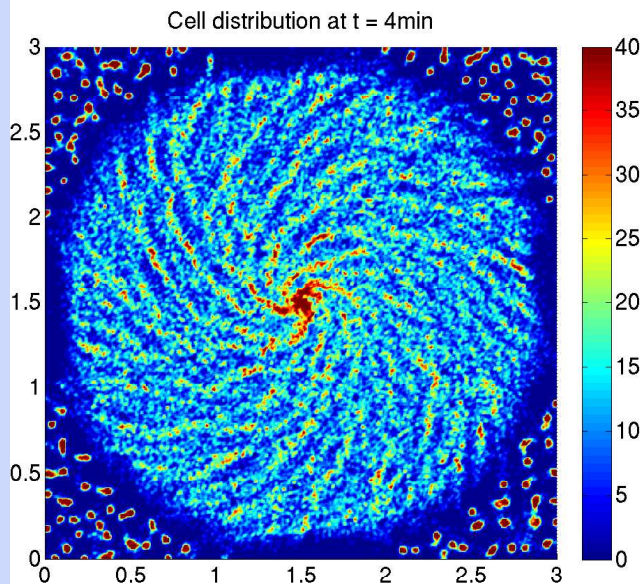
- Cell body length $1 - 2 \mu m \approx 10^{-6} m$
Cell “run” speed $10 \sim 30 \mu m/s \approx 10^{-5} m/s$
If we use viscosity of water $\nu \approx 10^{-6} m^2/s$ at $20^\circ C$
- For a typical bacterium the Reynolds number $Re = UL/\nu \approx 10^{-5}$, so one can use the Stokes approximation
- Theoretically, after solving the Stokes equations for (\mathbf{u}, p) , we can calculate the torque and force acting on each cell, but not for many cells.
- We simplify all this by assuming cells are well separated, and incorporate a constant bias to the right in the cell velocity:

The bias and cell tracks

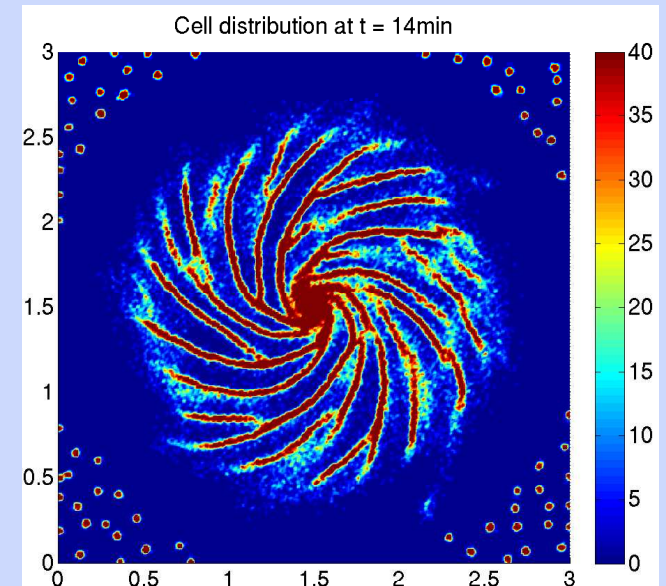
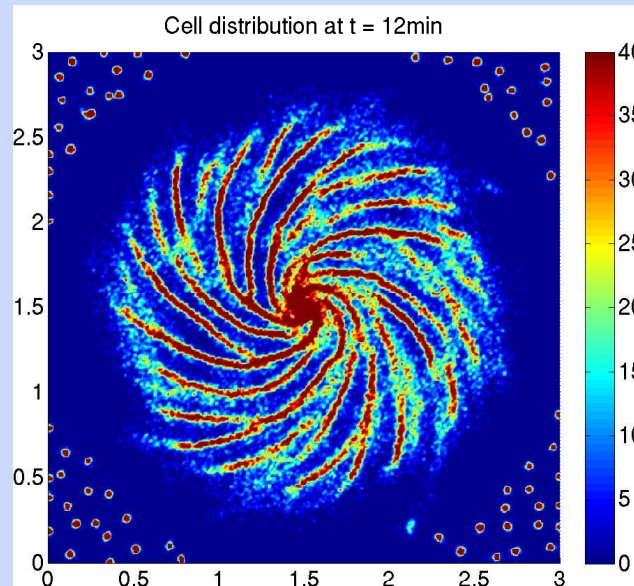
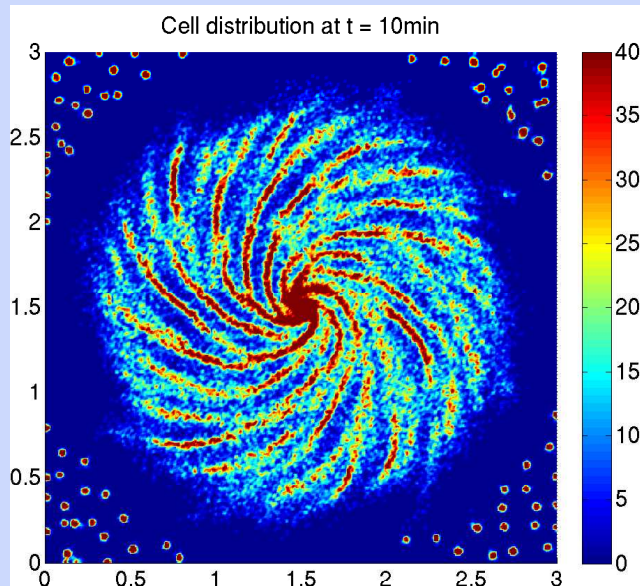
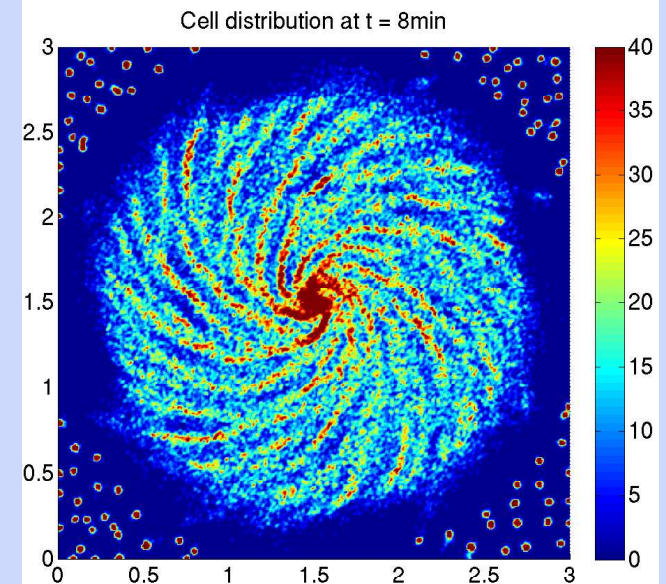
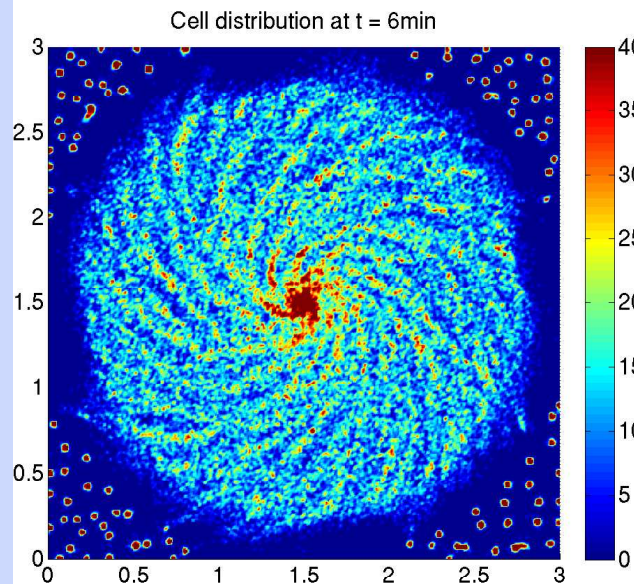
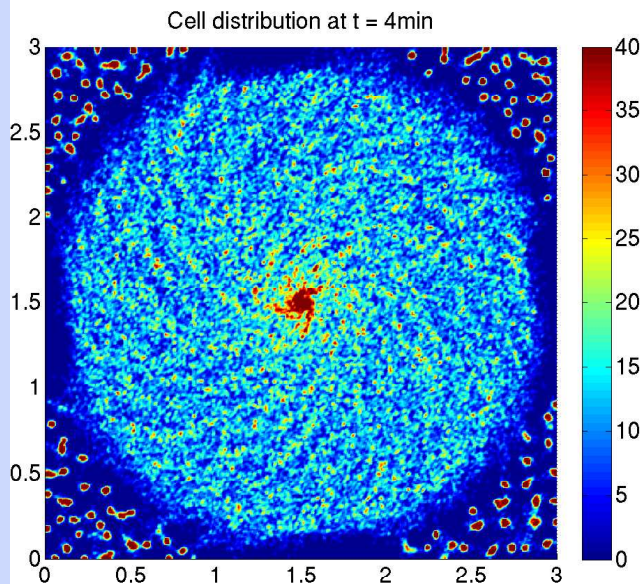
$$\frac{d\mathbf{v}}{dt} = \varepsilon_b \frac{\mathbf{v}}{|\mathbf{v}|} \times \mathbf{n}$$



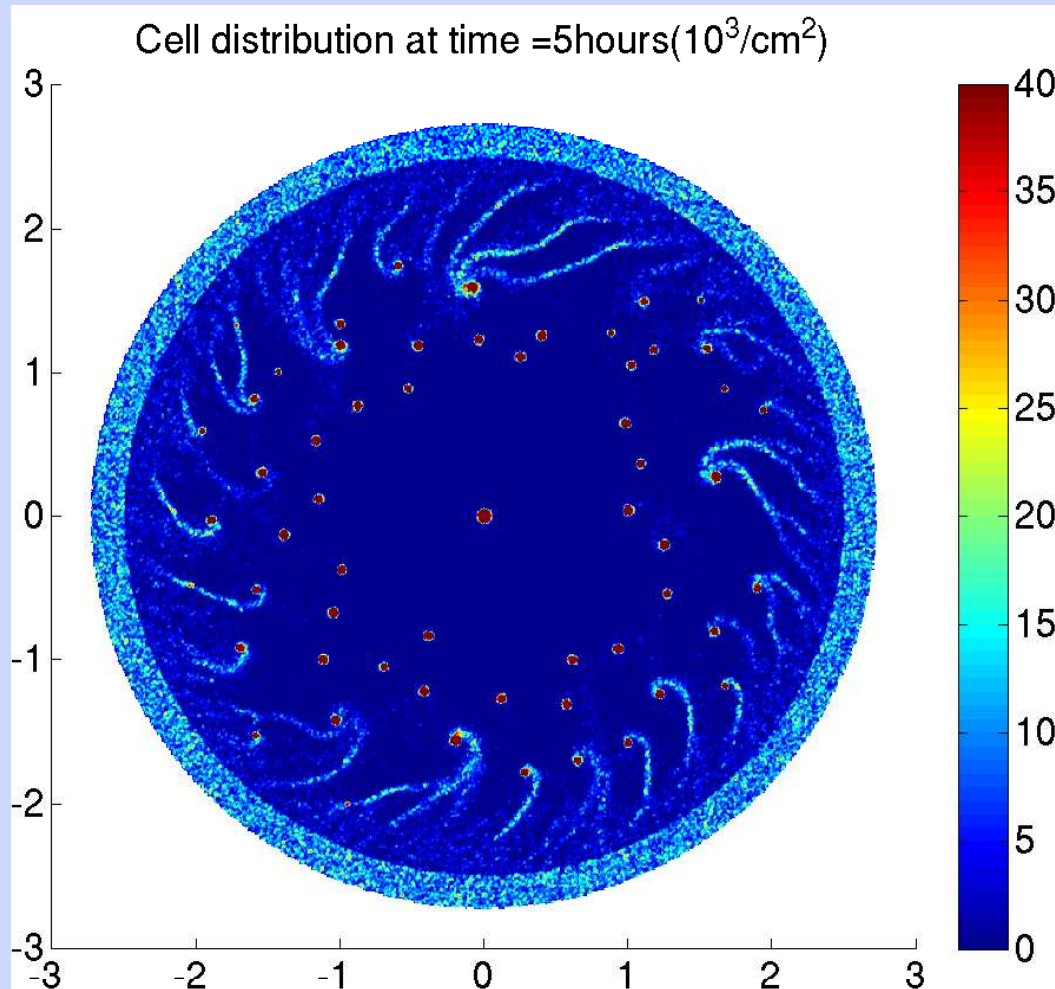
Spiral streaming



Spiral streaming - 2



Comparison with experimental results



Swimming near a surface leads to ..

If the torque on a cell is given by $F = \omega_0 v \times \nu$, then

$$\frac{\partial}{\partial t} n = D_n \Delta n - \nabla \cdot [G'(S) n (\chi_0 \nabla S + \beta_0 (\nabla S)^\perp)],$$

where

$$D_n = \frac{s^2}{2\lambda_0(1 - \psi_d) + \frac{2\omega_0^2}{\lambda_0(1 - \psi_d)}},$$

$$\chi_0 = \frac{a_1 s^2 (1 - \psi_d) [\lambda_0 (1 - \psi_d) (\lambda_0 (1 - \psi_d) + \frac{1}{t_a}) - \omega_0^2]}{2((\lambda_0 (1 - \psi_d) + \frac{1}{t_a})^2 + \omega_0^2)(\lambda_0^2 (1 - \psi_d)^2 + \omega_0^2)},$$

$$\beta_0 = \frac{\omega_0 a_1 s^2 (1 - \psi_d) (2\lambda_0 (1 - \psi_d) + \frac{1}{t_a})}{2((\lambda_0 (1 - \psi_d) + \frac{1}{t_a})^2 + \omega_0^2)(\lambda_0^2 (1 - \psi_d)^2 + \omega_0^2)},$$

and

$$\nabla S = \begin{pmatrix} \frac{\partial S}{\partial x_1} \\ \frac{\partial S}{\partial x_2} \end{pmatrix}, \quad (\nabla S)^\perp = \begin{bmatrix} 0 & 1 \\ -1 & 0 \end{bmatrix} \nabla S.$$

The continuum model applied to bacterial patterns

- The cell density is described by the chemotaxis equation

$$\frac{\partial n}{\partial t} = \nabla \cdot (D_n \nabla n - \chi n \nabla S) + g(n, f) \quad \text{in } D \times \mathbb{R}^+$$

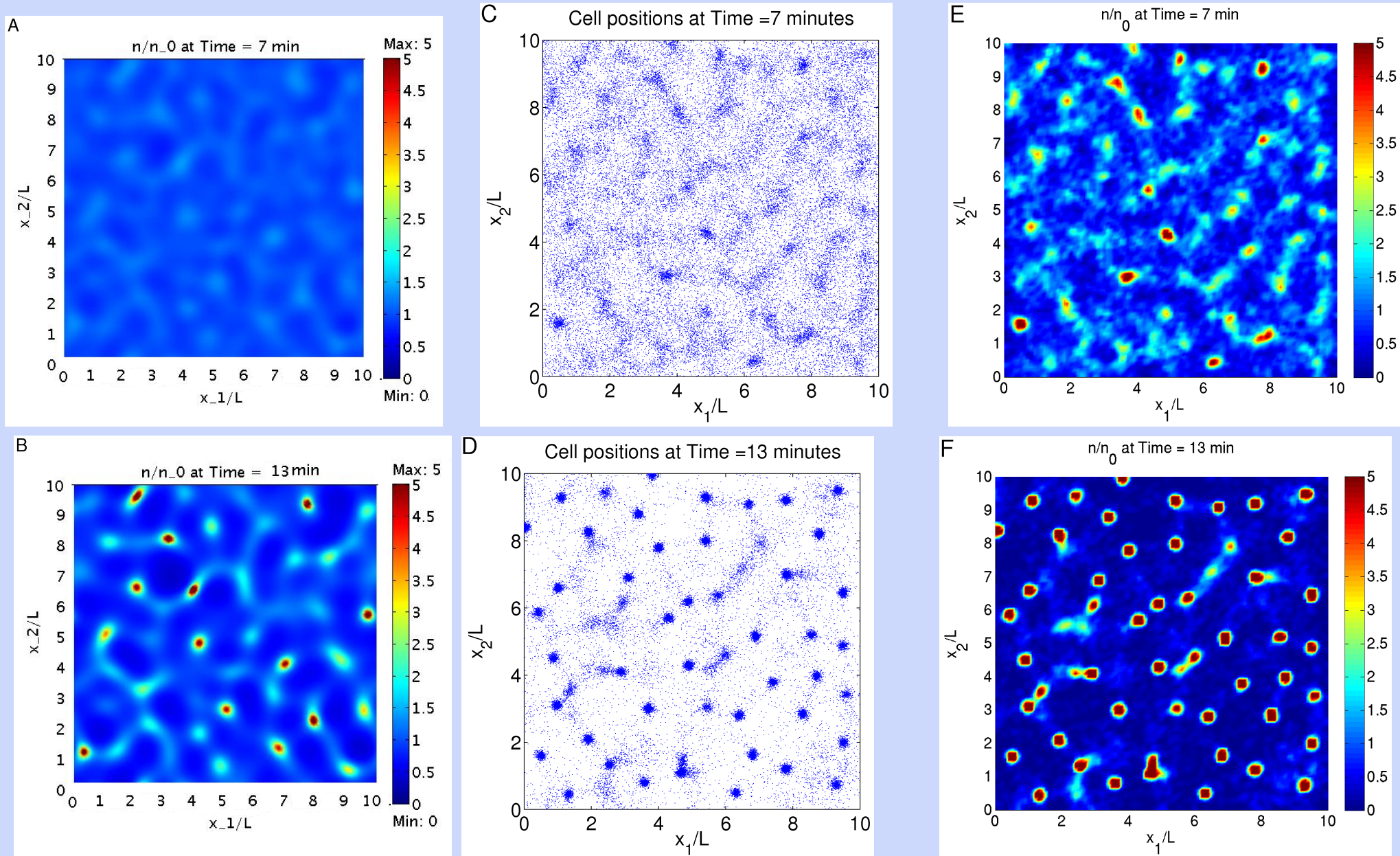
where the chemotactic sensitivity is computed according to the preceding analysis.

- The chemical fields are described by a system of reaction-diffusion equations

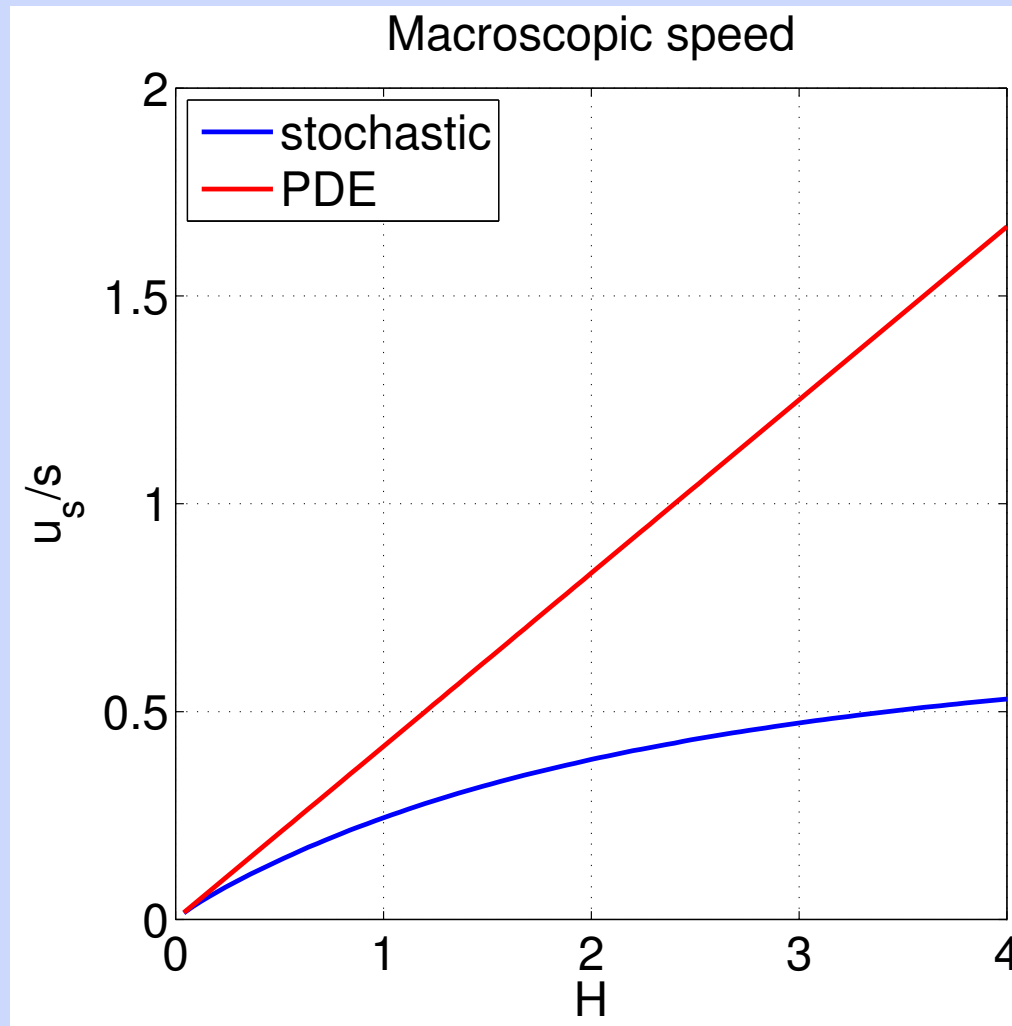
$$\begin{aligned} \frac{\partial S}{\partial t} &= \nabla \cdot (D_S \nabla S) + \gamma n - \mu S \quad \text{in } D \times \mathbb{R}^+ \\ \frac{\partial f}{\partial t} &= \nabla \cdot (D_f \nabla f) - u(n) \quad \text{in } D \times \mathbb{R}^+ \end{aligned}$$

- Neumann boundary conditions are imposed on both cells and chemicals.

Pattern formation ...



Problems with large gradients



C. Xue, E. Budrene and H. G. Othmer, Radial and spiral stream formation in *Proteus mirabilis* colonies, PLoS Comp Biol, 7, 1-11, (2011).

Some insight into why it doesn't work ..

Recall the internal dynamics

$$\frac{dz_1}{dt} = \frac{-z_1 - z_2}{t_e}$$

$$\frac{dz_2}{dt} = -\frac{z_2}{t_a} - G'(S(x(t), t)) \left(\nabla S \cdot \mathbf{v} + \frac{\partial S}{\partial t} \right)$$

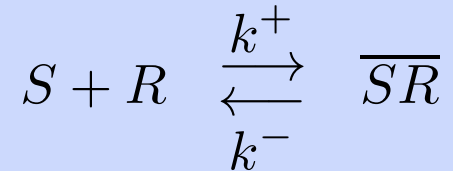
and the chemotactic velocity

$$\left[\frac{a_1 s}{N\lambda_0(1 + (1 - \psi_d)t_a\lambda_0)(1 + (1 - \psi_d)t_e\lambda_0)} \right] st_a G'(S) \nabla S$$

Thus if the Lagrangian derivative of the signal is too large the internal state cannot adapt rapidly enough. In principal one simply has to retain higher moments, as the following show.

But there is a phenomenological 'solution' to this ..

A phenomenological fix ..



The evolution equation for the bound receptor density is

$$\frac{d}{dt} \overline{SR} = k^+ S \cdot R_0 - (k^+ S + k^-) \overline{SR} \quad (3)$$

The input G can be taken as proportional to the fraction of receptors occupied

$$G(S) = G_0 \left(\frac{S}{K_D + S} \right) \quad (4)$$

where $K_D = k^- / k^+$. We have to compare the time scales

$$\tau_{sig} \equiv \frac{S}{s|\nabla S|} \quad \tau_{rec} \equiv \frac{1}{k^+ S + k^-}$$

and if $\tau_{sig} < \tau_{rec}$ then the equilibration assumption is not valid since the receptors cannot process the signal.

A phenomenological fix ..

Define the rates of change

$$\frac{\delta S}{\delta t}_{(sig)} \equiv \frac{s|\nabla S|}{S}$$

and

$$\frac{\delta S}{\delta t}_{(rec)} \equiv \frac{S}{k^+ S + k^-}$$

A more ‘correct’ Lagrangian derivative of the signal, which appears in the analysis using the cartoon model, is

$$\min\{s\nabla S, (k^+ S + k^-)S\} \quad (5)$$

Of course the min function is difficult to handle analytically, so an alternate form that captures the essential properties is

$$\frac{1}{\frac{1}{\Omega} + \frac{1}{s\nabla S}} = \frac{s\Omega\nabla S}{\Omega + s|\nabla S|}$$

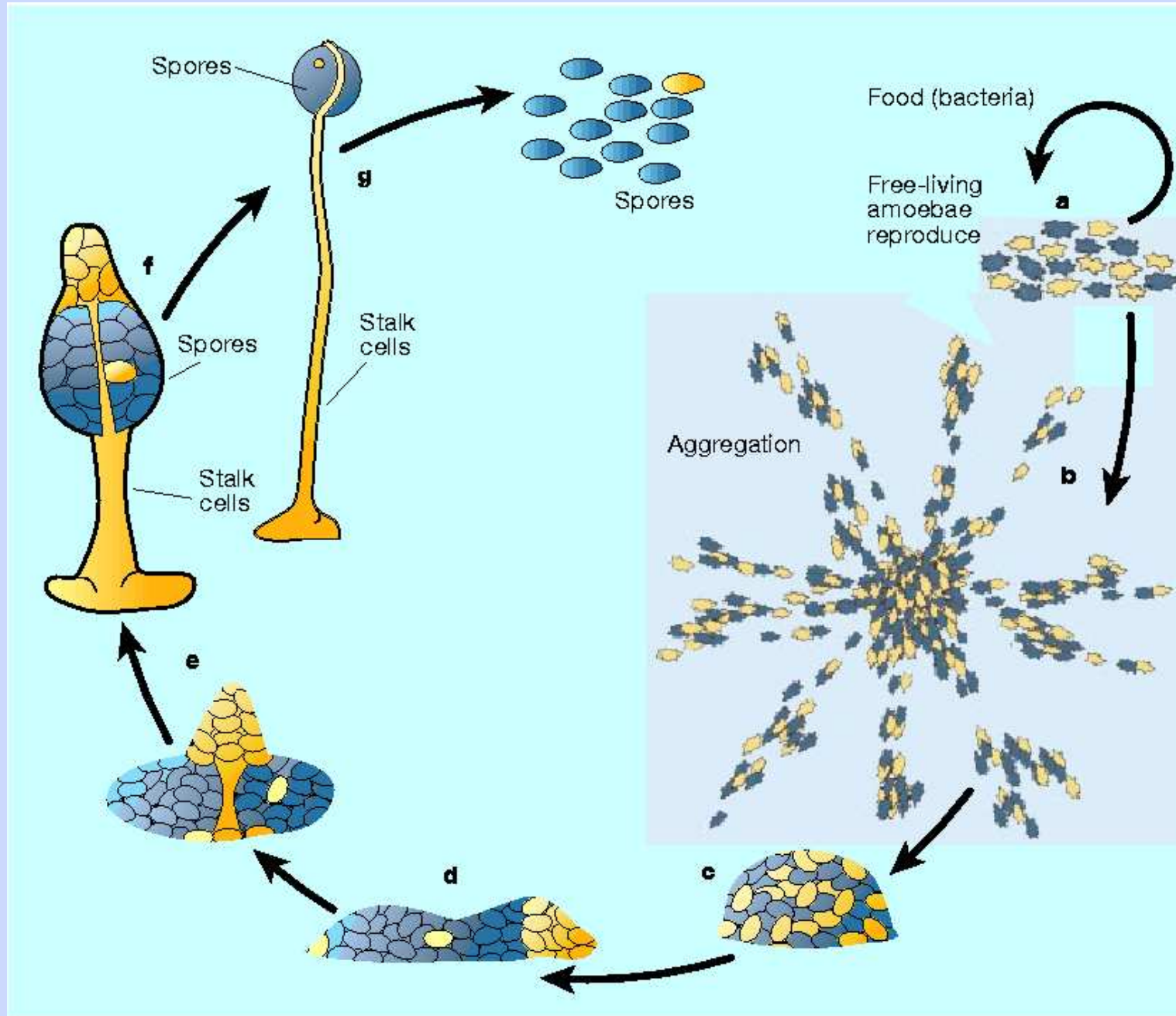
wherein

$$\Omega \equiv (k^+ S + k^-)S.$$

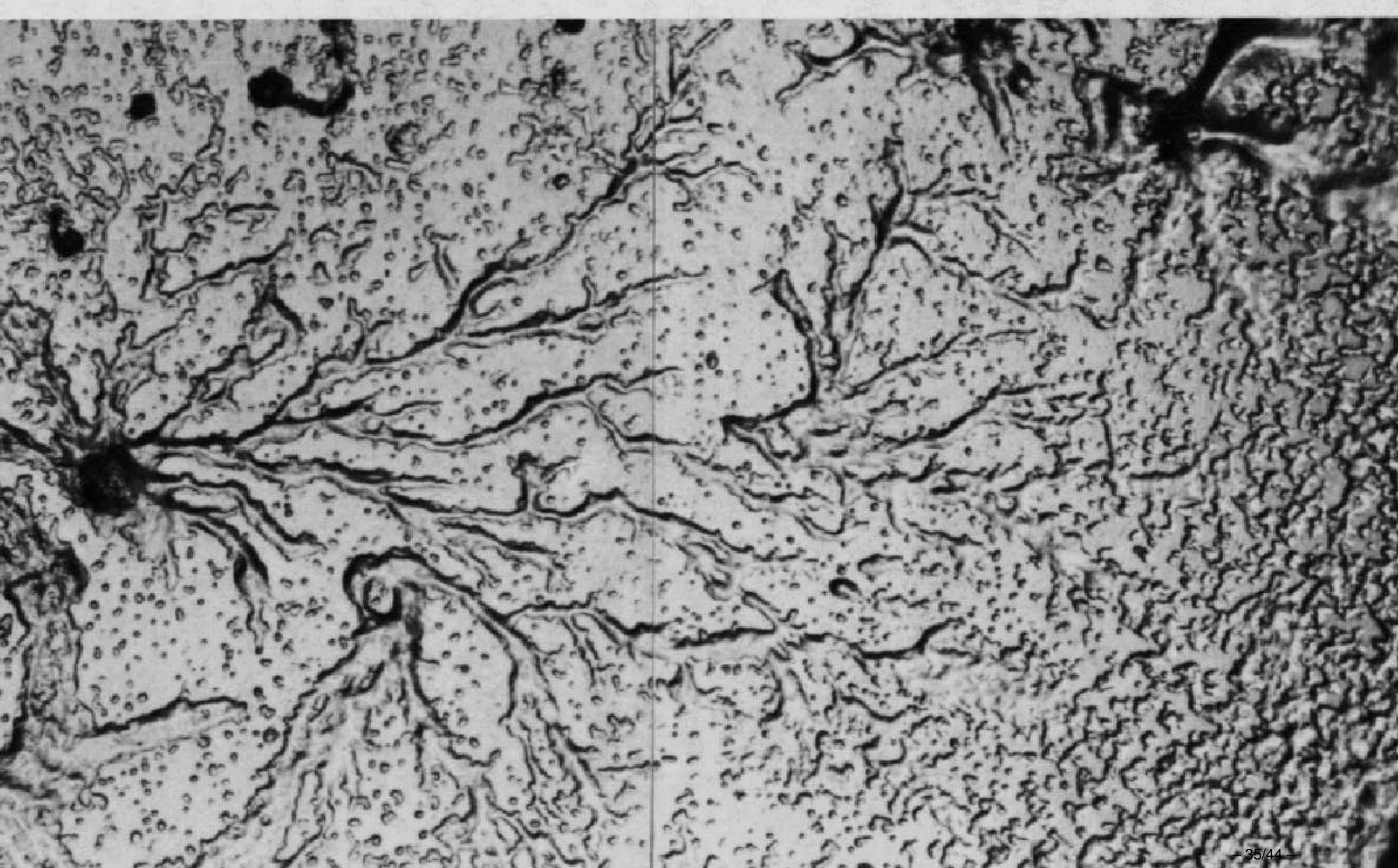
The amoeboid problem –

– crawling is harder than swimming!

The life cycle of *Dictyostelium discoideum*



Aggregation patterns



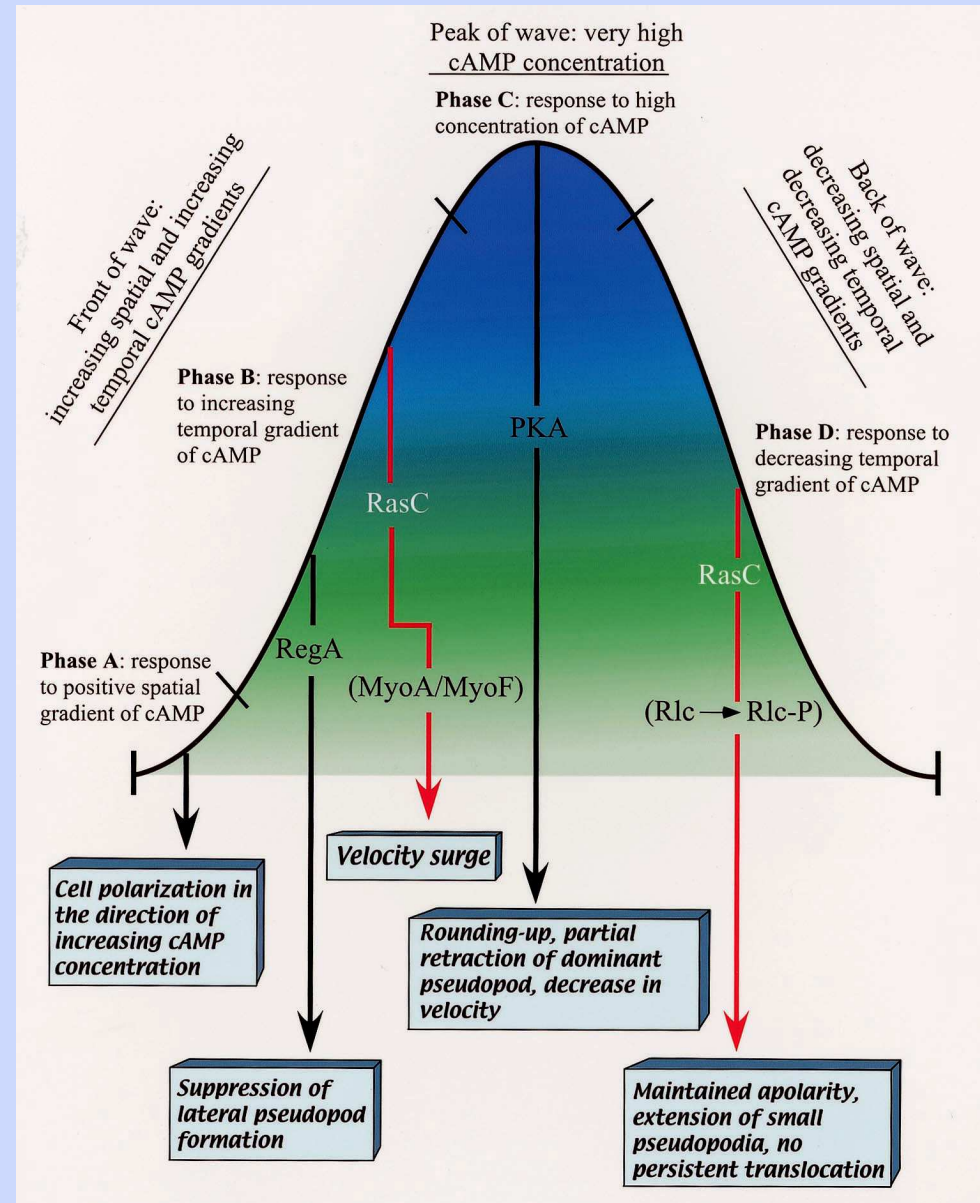
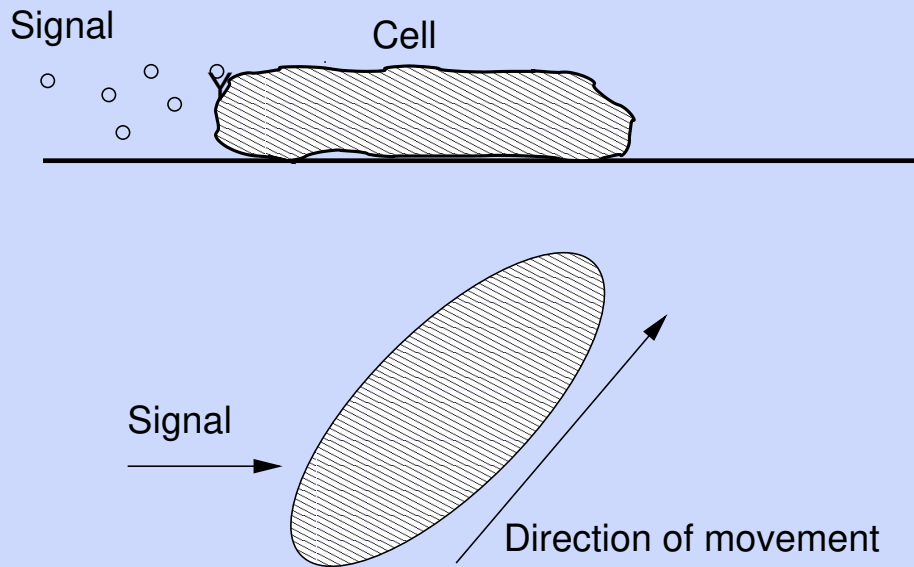
How do we model and analyze these behaviors, and what do we learn from that process?

What cellular-level processes are involved in producing the population-level aggregation patterns, or in other words, what must a cell do to have a chance of passing on its genes?

- Some cells (or small groups of cells) must become pacemakers
- A cell must detect the external signal cyclic adenosine 3',5'-monophosphate (cAMP)
- It must choose a direction in which to move
- Cells must amplify and relay the signal, and adapt to the ambient signal
- They must move for an appropriate length of time
- Eventually a cell interacts with its neighbors and moves collectively, first in pairs, then in streams, ..
- Slightly later it has to 'decide' what type of cell to become in the final fruiting body. This is a collective decision reached by the community (absent cheaters!).
- The entire aggregate has to stop migrating and erect the fruiting body

Orientation and movement in a wave

In an aggregation wave ...

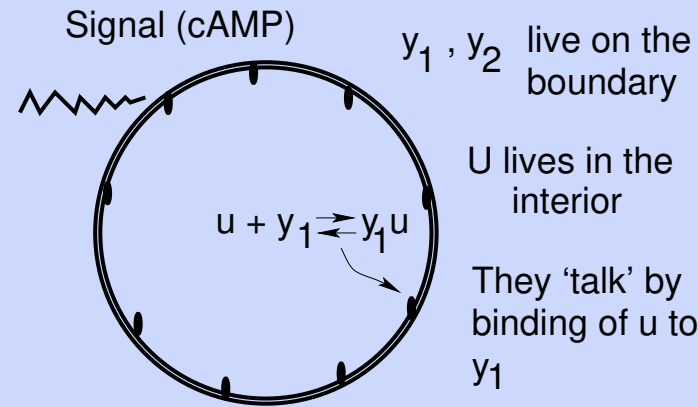


AND ... A cell also stimulates itself when it signals!

Some basic questions concerning direction sensing and polarization

- What is the source of the sensitivity and amplification (cells can respond to differences as small as 2% front-to-back and produce a much larger –estimated to be six-fold– intracellular gradient)?
- What is the role of actin polymerization in the amplification and the ‘imprinting’ of directionality?
- What are the long-term morphological changes that characterize polarization?
- How do we model these processes at a microscopic level? Are stochastic effects negligible, important, dominant ..? Note that forces and the motile machinery that generates them are crucial here.
- Can we embed the microscopic processes/models in useful macroscopic equations?

A spatially-distributed cartoon model



$$\frac{dy_1}{d\tau} = \frac{S(\tau) - (y_1 + y_2)}{\tau_e} - k^+ y_1 u + k^- y_1^- u$$

$$\frac{dy_2}{d\tau} = \frac{S(\tau) - y_2}{\tau_a}$$

$$\frac{\partial u}{\partial \tau} = \Delta u \quad \text{in } \Omega$$

$$-D \frac{\partial u}{\partial n} = k^+ y_1 u - k^- y_1^- u \quad \text{on } \partial\Omega$$

How does one define a transport equation when the internal state lives in a Banach space?

Signal transduction for orientation ..

$$\begin{aligned}\frac{\partial y_1}{\partial t}(\theta, t) &= \frac{S(\theta, t) - y_1(\theta, t) - y_2(\theta, t)}{t_e} \\ \frac{\partial y_2}{\partial t}(\theta, t) &= \frac{S(\theta, t) - y_2(\theta, t)}{t_a}\end{aligned}$$

Let $x = (x_1, x_2)$ be the centroid position and write

$$S(\theta, t) = S(x_1 + R_0 \cos \theta, x_2 + R_0 \sin \theta, t)$$

$$S(\theta, t) \sim S(x) + R_0 \cos \theta \frac{\partial S}{\partial x_1}(x) + R_0 \sin \theta \frac{\partial S}{\partial x_2}(x)$$

$$\begin{pmatrix} p_0(x, t) \\ q_0(x, t) \\ q_1(x, t) \\ q_2(x, t) \end{pmatrix} = \int_0^{2\pi} \begin{pmatrix} y_1 \\ y_2 \\ y_2 \cos \theta \\ y_2 \sin \theta \end{pmatrix} d\theta$$

Moving cells ..

$$\frac{dq_0}{dt} = \frac{2\pi S(x) - q_0}{t_a}$$

$$\frac{dq_1}{dt} = \frac{R_0\pi \frac{\partial S}{\partial x_1}(x) - q_1}{t_a}$$

$$\frac{dq_2}{dt} = \frac{R_0\pi \frac{\partial S}{\partial x_2}(x) - q_2}{t_a}$$

$$\frac{dp_0}{dt} = 2\pi \frac{\partial S}{\partial x_1}(x)v_1 + 2\pi \frac{\partial S}{\partial x_2}(x)v_2 + 2\pi \frac{\partial S}{\partial t}(x) - \frac{p_0}{t_a}$$

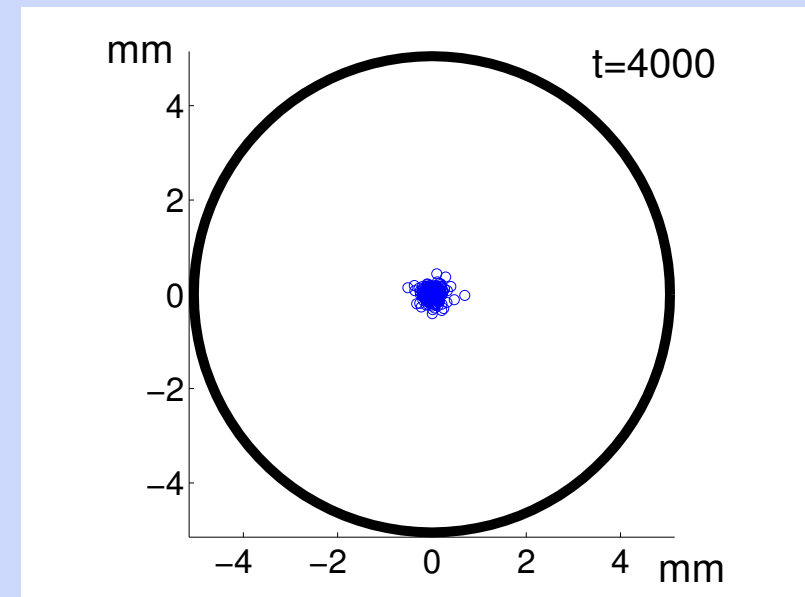
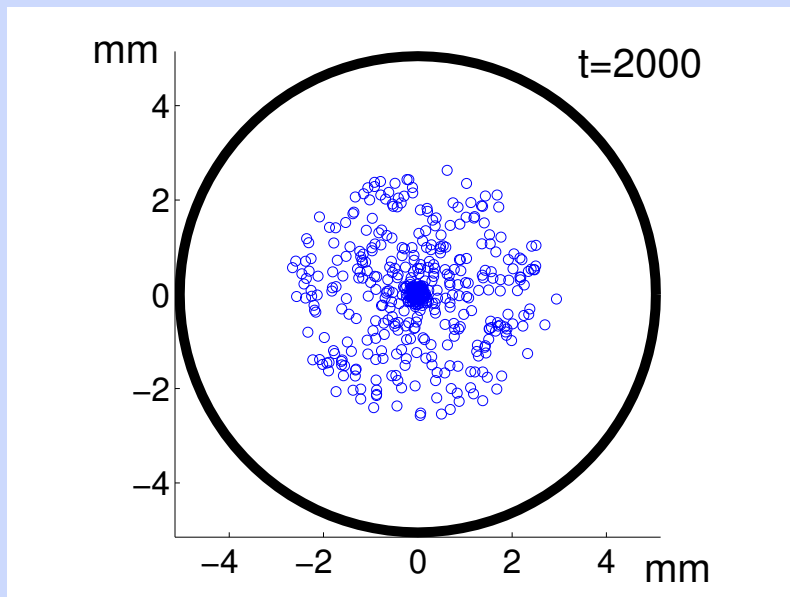
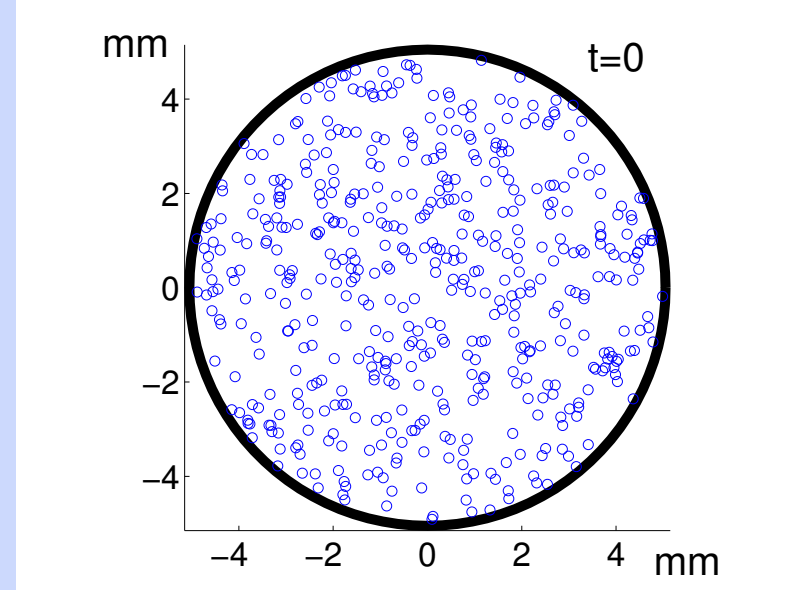
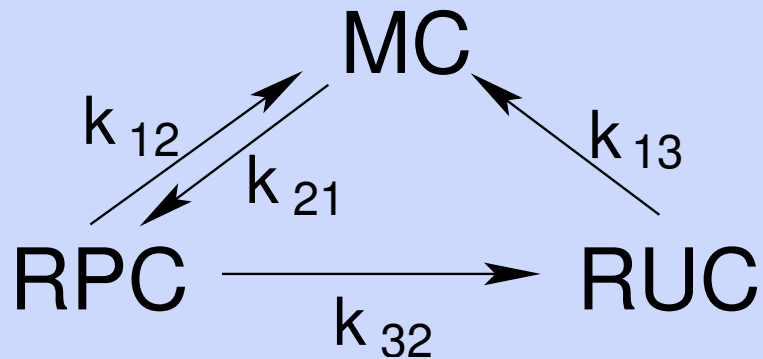
$$\frac{dx_1}{dt} = v_1 \quad \frac{dx_2}{dt} = v_2.$$

Newton's Law

$$\frac{dv_1}{dt} = \frac{\gamma q_1 - v_1}{t_d} \quad \frac{dv_2}{dt} = \frac{\gamma q_2 - v_2}{t_d}$$

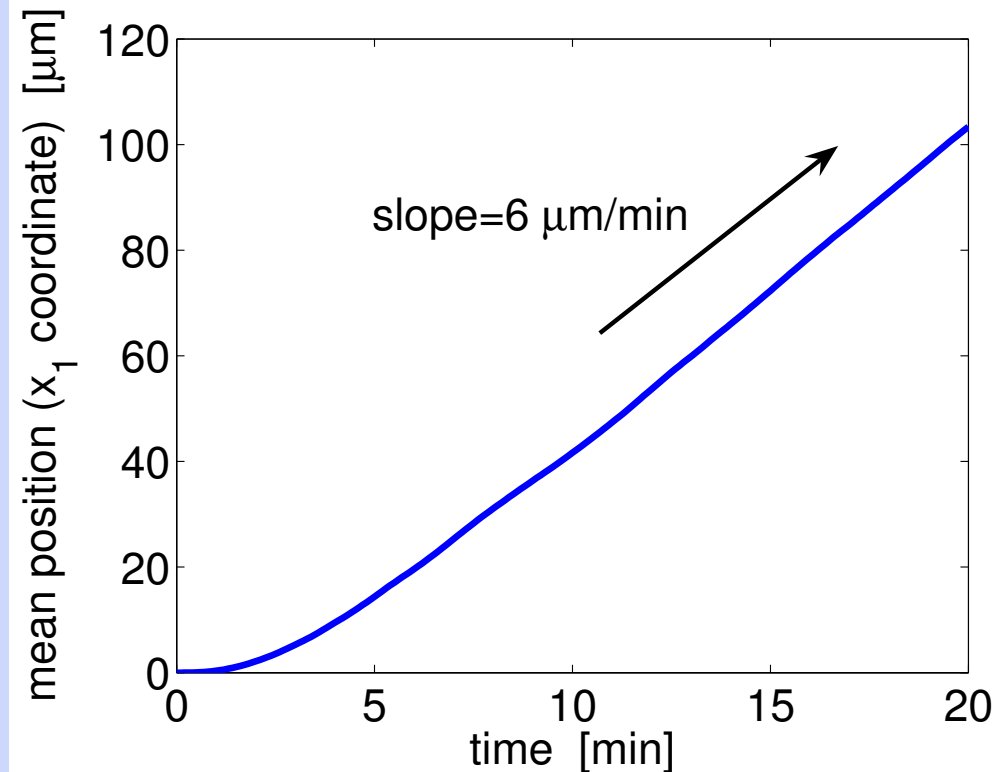
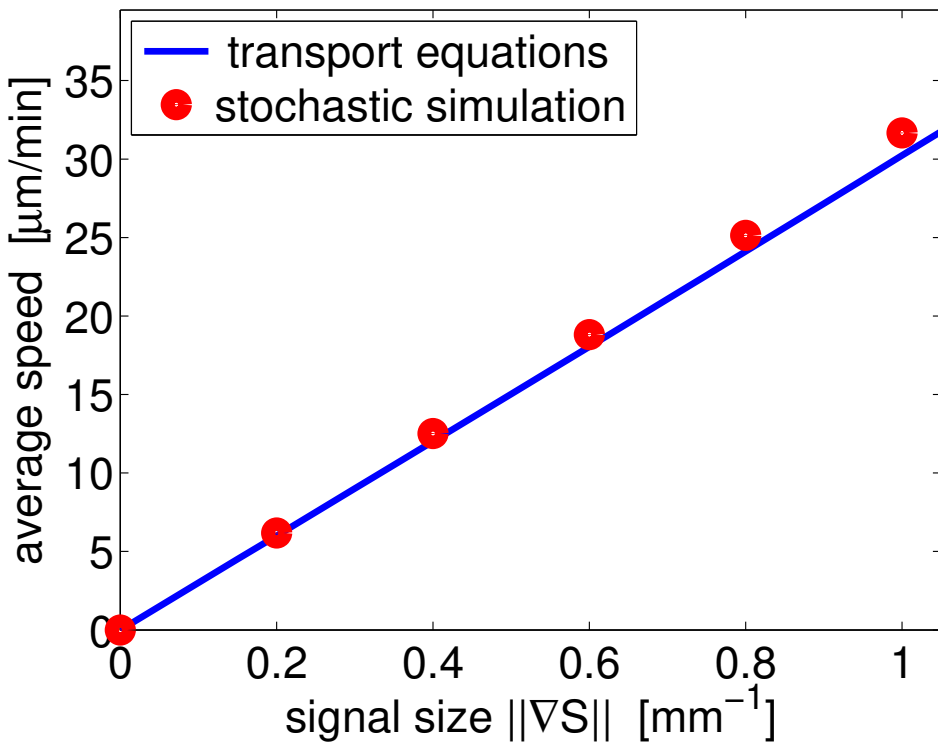
This suffices for a steady gradient, but doesn't solve the back-of-the-wave problem.

For that we introduce resting states...



This solves the back of the wave problem.

Comparison of predictions



Radek Erban and Hans G. Othmer Taxis equations for amoeboid cells, J. Math. Biol., 54, 847-885, (2007).

Conclusions ..

- For simple systems such as bacteria one can derive PKS equations from the transport equation with internal state variables, and thereby derive the chemotactic sensitivity in terms of characteristics of the microscopic motion.
- For amoeboid cells such as Dd, its harder to obtain reduced equations, but the moment equations reflect the population-level behavior well.
- Whether PKS can be obtained from the transport equations is still open ...